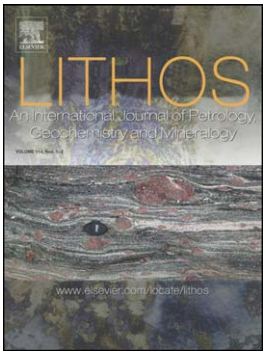

Jurassic arc volcanism on Crimea (Ukraine): Implications for the paleo-subduction zone configuration of the Black Sea region

M.J.M Meijers, B. Vrouwe, D.J.J. van Hinsbergen, K.F. Kuiper, J. Wijbrans, G.R. Davies, R.A. Stephenson, N. Kaymakcı, L. Matenco, A. Saintot

PII: S0024-4937(10)00193-3
DOI: doi: 10.1016/j.lithos.2010.07.017
Reference: LITHOS 2277

To appear in: *LITHOS*

Received date: 28 January 2010
Accepted date: 19 July 2010

Please cite this article as: Meijers, M.J.M., Vrouwe, B., van Hinsbergen, D.J.J., Kuiper, K.F., Wijbrans, J., Davies, G.R., Stephenson, R.A., Kaymakcı, N., Matenco, L., Saintot, A., Jurassic arc volcanism on Crimea (Ukraine): Implications for the paleo-subduction zone configuration of the Black Sea region, *LITHOS* (2010), doi: 10.1016/j.lithos.2010.07.017

Jurassic arc volcanism on Crimea (Ukraine): implications for the paleo-subduction zone configuration of the Black Sea region

M.J.M Meijers[1,2], B. Vrouwe[2], D.J.J. van Hinsbergen[1,3], K.F. Kuiper[1,2], J. Wijbrans[2], G.R. Davies[2], R.A. Stephenson[4], N. Kaymakcı[5], L. Matenco[2], A. Saintot[6]

[1]Dept. of Earth Sciences, Utrecht University, Budapestlaan 17, 3584 CD Utrecht, The Netherlands

[2] Faculty of Earth and Life Sciences, VU University Amsterdam, De Boelelaan 1085, 1081 HV Amsterdam, The Netherlands

[3] Physics of Geological Processes (PGP), University of Oslo, Physics building, Sem Sælands vei 24, 0316 Oslo, Norway

[4] School of Geosciences, University of Aberdeen, Meston Building, King's College, Aberdeen AB24 3UE, United Kingdom

[5] Dept. of Geological Engineering, Faculty of Engineering, Middle East Technical University, İnönü Bulvarı, 06531-Ankara, Turkey

[6] Geological Survey of Norway, NGU, Leiv Eirikssons vei 39, 7491 Trondheim, Norway

Abstract

The early Cretaceous and younger opening of the Black Sea has obliterated much of the older record of Tethyan subduction below southeastern Europe. The earlier Mesozoic evolution was dominated by opening and closure of Tethyan oceans between Gondwana and Laurasia with their consumption, at least in part, accommodated along the southern Eurasian margin. Crimea (Ukraine), a peninsula in the northern Black Sea, represents the northernmost region of southeastern Europe that exposes a record of a pre-Cretaceous Tethyan active margin. To shed new light on the paleosubduction zone configuration of

the southeastern European margin in the Jurassic, we report $^{40}Ar/^{39}Ar$ isotope dating on 10 samples and whole rock geochemistry on 31 samples from supposedly Jurassic magmatic rocks from the Crimean peninsula. The samples can be subdivided into two age groups: middle Jurassic (~172-158 Ma) and uppermost Jurassic to lowermost Cretaceous (~151-142 Ma), that both have a subduction-related geochemical signature. The ages of the younger group are in conflict with previously assigned biostratigraphic ages of the units under-and overlying the volcanic complex. This might suggest a scenario where the latter were juxtaposed by faulting. We argue that the Crimean volcanics represent a fragment of a volcanic arc overlying the southeastern European continental margin. These data therefore provide evidence for Jurassic northwards subduction below the Eurasian margin, preceding the opening of the Black Sea as a back-arc basin. We argue that the corresponding Jurassic trench was already positioned south of the Turkish Pontides and the Caucasus belt, implying a very shallow slab angle in the Jurassic.

1. Introduction

Much remains to be understood about the Mesozoic configuration of subduction zones in the present-day Black Sea region. Fundamentally different views on the number, as well as the location and polarity of subduction zones in this region in Jurassic times prevail in the literature (Barrier and Vrielynck, 2008; Dercourt et al., 2000; Kazmin et al., 1987; Kent and May, 1987; Moix et al., 2008; Robertson and Dixon, 1984; Şengör and Yilmaz, 1981; Stampfli and Borel, 2002). Geodynamic reconstructions display a complex subduction zone configuration in the present-day eastern Mediterranean region (Figs. 1 and 2), resulting from two simultaneously interacting large-scale plate tectonic processes: 1) the early stages of Pangea break-up by opening of the central Atlantic ocean, imposing a widely dispersed sinistral strike-slip movement of Laurasia to the north relative to Gondwana to the south (Favre and Stampfli, 1992; Stampfli and Borel, 2004), and 2) south-to-north motion of blocks rifting away from Africa, accommodated by subduction of the (Paleo- and Neo-) Tethys oceans beneath the southern Eurasian margin (Fig. 2) (Şengör and Yilmaz, 1981). The Jurassic paleo-position of the subduction zones and continental blocks along the southern Eurasian margin in the present-day Black Sea region, however, is poorly constrained, because opening of the Black Sea since the early

Cretaceous has obscured much of the geological record. A key area in the present-day Black Sea region is the Crimean peninsula. Here, heavily deformed Triassic-lower Jurassic turbiditic sediments are covered by an upper Jurassic carbonate platform (Mileyev et al., 1997; Voznesensky et al., 1998). Magmatic intrusions that are observed within the Triassic-lower Jurassic sequence are of unknown geochemical composition. Whether these magmatic intrusions and associated extrusive volcanism along the southern European margin relate to rifting in a back-arc setting or locate the volcanic arc of a Jurassic subduction zone is a matter of debate (Nikishin et al., 2001; Saintot et al., 2006b; Saintot et al., 2007). Here, we provide critical constraints on the genesis of Jurassic magmatism on Crimea. To this end, we carried out $^{40}Ar/^{39}Ar$ isotope dating and major and trace element X-ray fluorescence (XRF) analysis on supposedly Jurassic Crimean volcanics. The results will be used to infer the plate tectonic setting for Crimea during volcanism, and we place this interpretation in context with respect to the Greater Caucasus and Turkish Pontides.

2. Geological setting

2.1 Main geological units in the circum-Black Sea region

The circum-Black Sea region contains a number of continental terranes and oceanic units, which are briefly reviewed here.

In northern Turkey, three continental units are combined into the **Pontides** belt. This belt comprises the Strandja Massif and the İstanbul Zone in the west, the bulk is represented by the Sakarya Zone (Fig. 1) (Okay et al., 1996). The Pontides are bounded in the north by the Black Sea and in the south by the İzmir-Ankara-Erzincan ophiolitic suture zone. The İstanbul Zone is structurally the highest zone, and the Sakarya Zone is structurally the lowest zone (Okay et al., 2001a). For the purpose of this study, we will only describe the Istanbul and Sakarya Zones.

The **İstanbul Zone** comprises non-metamorphic Paleozoic, Mesozoic and Cenozoic sedimentary sequences overlying pan-African/Cadomian crystalline basement (Chen et al., 2002; Ustaömer et al., 2005). The Paleozoic affinity of the İstanbul zone is debated (Chen et al., 2002), but there is general concensus based on its stratigraphy and lack of metamorphism – that in Mesozoic times it can be considered as a fragment of

Moesia that rifted southward during the opening of the western Black Sea basin in the late Cretaceous (Okay et al., 1994; Üstaömer and Robertson, 1993).

The **Sakarya Zone** has a crystalline basement with Carboniferous metamorphic ages (Bozkurt et al., 2008; Okay et al., 2008; Topuz and Altherr, 2004; Topuz et al., 2004; Topuz et al., 2007) and is overlain by the locally metamorphosed Karakaya Complex of Triassic to earliest Jurassic age, and a younger discordant Mesozoic to Cenozoic (volcano-)sedimentary cover (Chen et al., 2002; Ustaömer et al., 2005). Blueschists and eclogites have been recovered from the Karakaya complex, marking its affinity with a latest Triassic subduction zone (Okay and Monié, 1997; Okay et al., 2002). Triassic deposits present in the Karakaya Complex are either interpreted as an inverted (back-arc) rift basin or as a subduction accretion complex (Genç and Yilmaz, 1995; Okay and Göncüoğlu, 2004; Pickett and Robertson, 2004).

The Sakarya and İstanbul zones share a post-Triassic volcano-sedimentary cover. In the western and central Pontides lower Jurassic continental to shallow marine clastic rocks, intercalated with ammonitico-rosso levels are exposed (Altıner et al., 1991).The eastern part of the Sakarya Zone (i.e. the eastern Pontides) however, has a different lower to middle Jurassic stratigraphy, consisting of volcanics and volcano-sedimentary units (Yılmaz and Kandemir, 2006; Yılmaz et al., 2003), interpreted as related to a volcanic arc (Şen, 2007). The Mudurnu Formation that can be traced from the western to the eastern Pontides comprises turbidites and magmatic rocks of roughly middle Jurassic age (~Bajocian to Bathonian) (Altıner et al., 1991) and is interpreted as an equivalent of the eastern Pontides middle Jurassic volcanics and volcanoclastic by Genç and Tüysüz (2010). The tectonic setting wherein the magmatic rocks of the Mudurnu Formation is been under debate (Dokuz et al., 2006; Şen, 2007; Şengör and Yilmaz, 1981). The most recent study of Genç and Tüysüz (2010) proposes that the magmatic rocks were emplaced in an extensional basin situated on an active or just inactive subduction zone. Middle Jurassic (Callovian) to lower Cretaceous platform carbonates (İnaltı Formation) cover the entire Pontides (Görür, 1997; 2010; Tüysüz, 1999).

The İstanbul zone was once separated from the Sakarya Zone by the so-called **Intra-Pontide ocean** (Okay et al., 1994; Robertson and Üstaömer, 2004; Şengör and Yilmaz, 1981). The timing of opening and closure of the Intra-Pontide ocean, however,

remain controversial. Interpretations are based on the presence of metamorphosed sediments that are assumed to have been deposited in a Triassic rift, and on the presence of ophiolitic units. Opening of the ocean was proposed to range from Triassic to early Jurassic times, and closure may have started in Aptian-Albian times, coeval with the incipient rifting of the western Black Sea basin (Hippolyte et al., 2010; Okay et al., 1994; Robertson and Üstaömer, 2004; Şengör and Yilmaz, 1981). Based on ophiolite emplacement, the full closure of the Intra-Pontide suture is proposed to have occurred in late Cretaceous (Turonian) times (Robertson and Üstaömer, 2004). However, the ophiolitic units have also been interpreted as being part of the ophiolites that were formed in a single Mesozoic northern Neo-Tethys ocean. Emplacement of those 'so-called' Intra-Pontide ophiolites results from left-lateral strike slip according to Elmas and Yiğitbaş (2001). They argue that the similar post-middle Jurassic sedimentary cover of the Sakarya and İstanbul Zones evidences the juxtaposition of the two zones before the late Jurassic.

The eastern and western **Black Sea** basins are generally regarded as back-arc basins that opened resulting from Neo-Tethys subduction below the Pontides. Timing of the opening of the eastern Black Sea basin is not well constrained as a result of poor stratigraphic exposure, and estimates vary from early Cretaceous (Kriachtchevskaia et al., 2010; Nikishin et al., 2003) to early Cenozoic (Robinson et al., 1995; Robinson et al., 1996) and Eocene (Vincent et al., 2005). The western Black Sea basin opened in early Cretaceous times (Barremian-Albian) (Görür, 1997; Robinson et al., 1996; Tüysüz, 1999), and the interpretation of the Black Sea as a back-arc basin (Okay et al., 1994) would suggest northward subduction below the Pontides in this time span.

Since 90 Ma ophiolites were generated south of the Pontides, which were eventually emplaced onto continental crust of the Anatolide-Tauride and South Armenian blocks, which collided with the Pontides in Paleocene to Eocene times (Kaymakci et al., 2009; Şengör and Yilmaz, 1981; Sosson et al., In press). Prior to 90 Ma, the only post-Triassic accretion below the Pontides that can be attributed to northward subduction occurred in the so-called Kargı Massif in the center of the Pontides, where HP-LT metamorphic rocks with ages of 105 Ma and younger are found (Okay et al., 2006).

To the northeast of the eastern Pontides, the prominent **Greater Caucasus** fold-and-thrust belt is located (Fig. 1). The Greater Caucasus, of which Crimea is the western

prolongation, has basement formed by the Scythian Platform, i.e. the thinned margin of the East European Platform (Nikishin et al., 1996; Saintot et al., 2006b). The volcano-sedimentary cover of the Greater Caucasus is of Permian and younger age. Importantly, the Sinemurian/Pliensbachian to Aalenian are rift-related series, that include MORB-resembling tholeiitic basalts of Aalenian age (~173 Ma, that may be comparable to the rift-related sequences in the eastern Pontides (Lordkipanidze et al., 1989; Okay and Şahintürk, 1997). Banks and Robinson (1997) envisaged that this area was occupied by en-echelon sets of rhomb-shaped rift basins, situated at the southern Eurasian margin. The Bajocian is characterized by calc-alkaline lavas, comparable to those in the Transcaucasus area (Fig. 1) (Adamia et al., 1981). The Greater Caucasus middle Jurassic volcanics have a subduction-related signature. However, it has been proposed that the volcanics resulted from back-arc spreading in the vicinity of a subduction zone south of the Transcaucasus terrane in the Lesser Caucasus, or that the volcanic arc encompassed the Greater Caucasus in Bajocian times, due to a shallowing of the subducting slab, causing arc-volcanism ~200 km from the trench (McCann et al., 2010; Saintot et al., 2006a).

2.2 Plate tectonic history

There is some consensus as to the subduction zone configuration in the circum-Black Sea region prior to and following the Jurassic. In the late Triassic, the Anatolide-Tauride-South Armenian block (Fig. 1) - a continental terrane of African origin - rifted from the African margin, leading to the formation of intervening oceanic basins (Fig. 2) (Şengör and Yilmaz, 1981). This movement had roughly a south to north sense. Apparent polar wander paths display little net S-N convergence between Africa and Eurasia until 120 Ma (Besse and Courtillot, 2002; Torsvik et al., 2008), and the rifting away of terranes away from the northern African margin must therefore have been accommodated by consumption of the Neo-Tethyan oceanic lithosphere by subduction along the southern Eurasian margin. The Triassic Karakaya complex, either interpreted as an inverted (back-arc) rift basin or as a former subduction zone (Genç and Yilmaz, 1995; Okay and Göncüoğlu, 2004; Pickett and Robertson, 2004), probably represents this subduction

zone. This is further supported by the presence of Triassic blueschists (Bozkurt et al., 1997; Okay et al., 2002).

In Cretaceous times, there is evidence for northward subduction of Neo-Tethyan oceanic crust south of the Pontides, from ophiolitic fragments with metamorphic soles of 90 Ma and younger ages that are present within, as well as south of the east-west trending İzmir-Ankara-Erzincan suture zone (Çelik et al., 2006; Moix et al., 2008; Yalınız et al., 2000). A widespread record of a late Cretaceous and younger volcanic arc record is located in the Pontides (Hippolyte et al., 2010; Okay et al., 2001b; Rice et al., 2006).An indication for pre-90 Ma Cretaceous subduction below the Pontides comes from cooling ages of subduction-accretion material in the Kargı window (Fig. 1) in the central Pontides, suggesting northward subduction below the Pontides from at least as early as ~105 Ma ago (Okay et al., 2006).

Very different views, however, exist on the subduction zone configuration of the modern Black Sea region in the Jurassic. For example, Dercourt et al. (2000; 1993) and more recently Barrier and Vrielynck (2008) place the Pontides at the southern continental margin of Eurasia in Jurassic times until the Cretaceous initiation of opening of the Black Sea. Alternative reconstructions by Stampfli and Borel (2002), Robertson et al. (2004) and Moix et al. (2008) separate the Pontides in Triassic to middle Jurassic times from the continental Eurasian margin by the small oceanic Küre basin. Supposedly, this ocean closed during southward subduction in late Triassic-middle Jurassic times (Stampfli and Kozur, 2006).

2.3 Geology of Crimea

Overall, the Crimean mountains have a northward-tilted structure, exposing in the south a complete Triassic to Tertiary sedimentary sequence. Boreholes indicate that Crimea is underlain by Paleozoic and/or older Eurasian basement (Gerasimov, 1994; Kruglov and Tsypko, 1988; Letavin, 1980; Mazarovich and Mileev, 1989; Milanovsky, 1991; Muratov, 1969). Its basement is likely part of the Scythian platform, which is the thinned margin of the East European Platform (EEP) (Gorbatchev and Bogdanova, 1993; Saintot et al., 2006b; Stephenson et al., 2004). Although the overlying post-Paleozoic

stratigraphy, which is locally intruded by minor (sub-) volcanic series, has been intensely studied, a number of controversies still exist.

The base of the entire stratigraphic sequence is made up by the Tauric group that is Triassic to lower Jurassic in age. The Tauric group is a sequence of highly deformed shales with intercalations of silicolites and coarser turbiditic material in the upper part, generally interpreted as an accretionary prism scraped off during the subsequent stages of subduction (Khain, 1984; Koronovsky and Mileyev, 1974; Muratov et al., 1984). The Tauric group contains Paleozoic to Triassic olistoliths, mostly carbonates (Popadyuk and Smirnov, 1996), interpreted as material driven from the overriding plate during subduction. The turbiditic interval, dominated by sandstones in the upper part of the Tauric group, has been assigned middle Jurassic ages (Bajocian to Bathonian, possibly Callovian) (Lalomov, 2007; Muratov et al., 1984). The upper part changes to a large variety of clastic lithologies, such as coal or ooidic sandstones, mostly proximal littoral or continental. Northwards these lithologies grade to massive conglomerates (Lalomov, 2007), which indicates a syn-kinematic deposition coeval with the final stages of a regressive basin fill. Several levels in this middle Jurassic sequence contain massive influx of volcanoclastic material, which indicates the onset of magmatic activity.

The Triassic to middle Jurassic sequences are intruded by magmatic bodies that were previously dated as Bajocian, based on cross-cutting relationships and faunal evidence (Latyshev and Panov, 2008; Spiridonov et al., 1990a; Spiridonov et al., 1990b; Sysolin and Pravikova, 2008).

The middle Jurassic (Bajocian) magmatism comprises volcanic complexes (with hypabyssal intrusive and extrusive bodies) and isolated igneous rocks in the Bodrak and Pervomaisk-Ayu-Dag areas in the western and central Crimean mountains, as well as the Karadag volcanic complex in eastern Crimean mountains (Fig. 3a). The Karadag complex consists of a volcano-sedimentary succession that was dated as Bajocian-Callovian on the basis of Bajocian fauna that intercalate with the lower volcanic sequence, and Bathonian to lower Callovian fauna that are present within the overlying sedimentary sequence (Voznesensky et al., 1998). Page et al. (1998), Latyshev and Panov (2008) and Sysolin and Pravikova (2008) suggest a tholeiitic island-arc setting for the production of these

volcanics, based on geochemical analysis. Ages however, have not been confirmed by isotopic dating.

Renewed subsidence is recorded at the beginning of the late Jurassic by the deposition of nodular limestones and distal clastics, which cover massive conglomerates (Muratov et al., 1984; Robinson and Kerusov, 1997). The direct transition is often obscured, but in several places proximal sandy limestones precede the nodular limestones over an unconformity (Lalomov, 2007). Zonenshain et al. (1990) proposed that the pebbles of the conglomerates were derived from the Pontides. More recently, it was argued that the conglomerates were probably sourced from within the basin itself (Hein, 2005). A general regressive pattern is subsequently observed by the deposition of upper Kimmeridgian to lower Berriasian massive reefal limestones that commonly grade laterally into carbonatic lithologies, such as slope or inner lagoon deposits (Arkad'ev et al., 2006; Arkad'ev and Rogov, 2006; Baraboshkin, 2003; Krajewski and Olszewska, 2006; Muratov et al., 1984; Robinson et al., 1996). The upper Jurassic to lowermost Cretaceous (lower Berriasian) is folded and thrusted southwards, forming the present-day nappe structure of the Crimean mountains (Mileyev et al., 1995; Nikishin et al., 1998; Popadyuk and Smirnov, 1991).

This sequence is unconformably overlain by Neocomian marls and marly limestones, Aptian to Albian grey pelagic clays (Popadyuk and Smirnov, 1991), upper Cretaceous carbonates and chalk, Paleocene calcarenites and Eocene nummulitic limestones (Fisher et al., 2005; Nikishin et al., 2008; Popadyuk and Smirnov, 1996). This entire Cretaceous to Eocene sequence is coeval with the main rifting stages of the Black Sea (Okay et al., 1994; Zonenshain and Le Pichon, 1986) and is well exposed on the northern flank of the Crimean mountains as a result of post-Eocene northward tilting (~5º). At the beginning of the Oligocene a thick succession of black paper shales with a high organic content was deposited, which is widely known as the Maikop facies (Finetti et al., 1988; Hudson et al., 2008; Robinson et al., 1996; Stolyarov and Ivleva, 2006). The overlying clastic carbonatic Miocene sequence is mostly distributed on the northern flank of the Crimean monocline.

3. Analyses & Results

3.1 Sampling

We collected volcanic samples in the Bodrak/Simferopol area and from the Karadag volcanic edifice for isotopic dating and geochemical analysis (Fig. 3a). The samples were collected from intrusive rocks (plutonic bodies, hypabyssal sills and feeder dykes) and extrusive rocks (typically pillow lavas, rhyolitic nuées ardentes and columnar lava flows; Fig. 3b and c). Thirty-one samples were collected for XRF major and trace element analysis, and ten samples were selected for $^{40}Ar/^{39}Ar$ dating (Table 1).

3.2 $^{40}Ar/^{39}Ar$ dating

The ten freshest samples from the Crimean peninsula were selected for $^{40}Ar/^{39}Ar$ dating after microscope inspection (Figs. 4 and 5, Tables 1 and 2). Groundmass, plagioclase and biotite were separated using standard mineral separation techniques. All samples were first crushed and sieved. Plagioclase and biotite crystals (either 125-250 μm or 200-250 μm fractions, see Table 2) were separated using heavy liquid separation and a Frantz magnet separator, followed by mineral picking under the microscope. For groundmass (samples KA28b and FET4G) the 250-500 μm fraction was selected for analysis. For the groundmass of sample KA28b we performed heavy liquid separations using two separate density ranges: $2.70>\rho>2.66$ g/cm^3 and $\rho<2.66$ g/cm^3. For sample FET4G we used the density fraction of $2.90>\rho>2.70$ g/cm^3. All separated fractions were leached with 1 N HNO_3 for one hour in an ultrasonic bath to clean samples before final re-picking by hand.

From all samples ~18-30 mg of material was wrapped in aluminum foil and loaded in a 15 mm ID quartz vial. Only for samples KARS01 and KA28b (both groundmass samples) 6 mg and 3 mg of material was loaded respectively, due to low amounts of material available. Between each set of 5 samples and at top and bottom positions, the in-house Drachenfels sanidine standard (25.26 ± 0.03 Ma, modified from Wijbrans et al. (1995)) was used as neutron fluence monitor. The loaded quartz vial was irradiated for 18 hours in the Cd-lined RODEO P3 position of the High Flux Reactor in Petten, the Netherlands. $^{40}Ar/^{39}Ar$ incremental heating experiments were carried out at the VU University of Amsterdam, the Netherlands. Standards were fused using a Synrad 48-5 50W CO_2 laser. Samples were spread out evenly in a sample tray with 6 mm diameter holes and incrementally heated with a Raylase scan head as a beam delivery and diffuser

system. In total, we performed 13 incremental heating experiments, on either plagioclase (8), groundmass (4) or biotite (1). For two samples both plagioclase and groundmass was separated (KA28b and FET4G) to validate the obtained ages.

After purification the gas was analysed with a Mass Analyzer Products LTD 215-50 noble gas mass spectrometer. Beam intensities were measured in a peak-jumping mode in 0.5 mass intervals over the mass range 40-35.5 on a Balzers 217 secondary electron multiplier. After every four steps system blanks were measured. Mass discrimination was monitored by frequent analysis of aliquots of air. By interpolating between the individually measured standard using a second-order polynomial fitting the irradiation parameter *J* was determined for each unknown sample.

Ages were calculated using the in-house developed ArArCalc software (Koppers, 2002). All $^{40}Ar/^{39}Ar$ ages were calculated using Steiger and Jäger (1977) decay constants. Uncertainties are reported at the 2σ level and include the analytical error and error in irradiation parameter (*J*). Correction factors for neutron interference reactions are $2.7 \pm 0.03 \times 10^{-4}$ for $(^{36}Ar/^{37}Ar)_{Ca}$, $6.99 \pm 0.13 \times 10^{-4}$ for $(^{39}Ar/^{37}Ar)_{Ca}$ and $1.83 \pm 0.2 \times 10^{-2}$ for $(^{40}Ar/^{39}Ar)_{K}$.

The results of the $^{40}Ar/^{39}Ar$ analyses are summarized in Table 2 and Figure 4 and 5. Full analytical data are given in the Supplementary Data. All steps yielding less than 2% $^{39}Ar_k$ were excluded in incremental heating spectra, but are included in the full analytical data tables (Tables 1 and 2). To define a reliable plateau age; i) at least three successive incremental heating steps should be included for calculation of a plateau age. ii) The steps that are used to calculate the plateau ages should represent more than 50% of the total $^{39}Ar_k$ released (e.g. Fleck et al. 1977). The mean squared weighted deviation (MSWD) over the plateau steps is a measure for plateau homogeneity, and should ideally range between 1.0 and 2.5, this was however not always the case (Table 2). We also checked for a relatively constant K/Ca ratio in the successive included incremental heating steps. The $^{40}Ar/^{36}Ar$ ratio was monitored to assess excess argon in the system (i.e. within 2σ error of 295.5). If no plateau age could be calculated or the sample suffered from excess argon, an isochron age was determined. This was the case for samples CUKR3 and IKUCH7. For sample KARS01 we decided to use the plateau age, despite the somewhat high MSWD value (2.49), because of the poor determination of the inverse

isochron intercept (Table 2). The isotopic ages from the groundmass of both KA28b samples with different densities yielded comparable plateau ages (151 ± 3 Ma and 149 ± 2 Ma) that are likely to be high estimates of the true emplacement age because of a high initial $^{40}Ar/^{36}Ar$ ratio of 315.8 ± 6.9 that indicates the presence of excess ^{40}Ar. The data were combined in a single isochron age of 143 ± 2 Ma that we feel dates the emplacement event more reliably. From the remaining eleven processed samples, eight plateau ages and a single isochron age were calculated. The two fractions of groundmass of sample FET4G did not yield geologically meaningful results.

3.3 Geochemistry

Major and trace elements were determined from 31 samples by XRF measurements on fused glass beads and pressed powder pellets at the VU University Amsterdam. International standards are used for calibration and in-house samples run as internal monitors. Results are displayed in Table 3. Loss on ignition (LOI) where determined at 1000ºC to provide an indication of the degree of low temperature alteration. The LOI vary from 1.1 to 20.1%. The major element compositions of samples with LOI's higher than 6% (samples 3, 4, a6 and a16) are not considered further.

From the TAS classification diagram (Irvine and Baragar, 1971; Le Maître et al., 1989) (Fig. 6) a subalkaline to tholeiitic trend can be observed in the samples, that range in composition from basaltic andesites to dacites (older age group) and dacites to rhyolites (the two yellow triangles; younger age group, Karadag). The most mafic rock (a1) contains 8.6 wt% MgO and is a trachybasalt. The subalkaline to tholeiitic trend in the samples rules out the possibility that volcanism was related to early stages of rifting in, for example, a back arc environment, which would have produced alkaline volcanism. Moderately compatible trace element contents (REE, Sr, Zr etc.) have abundances comparable to E-MORB; i.e. in the range of 5-10 times that of primitive mantle (Sun and McDonough, 1989). In contrast, the large ion lithophile element (LILE, e.g. Rb, Ba and K) record significant variations but with most concentrations significantly higher than the E-MORB and the most mafic samples with >30 times primitive mantle. This general enrichment in LILE contrasts with that of the high field strength elements (HFSE, e.g. Nb), which is close to primitive mantle values in the more mafic samples and always

below E-MORB concentrations. The low Nb concentration compared to the LILE and LREE is a characteristic of subduction-related volcanism. In a Ce/Nb versus Zr diagram (Fig. 7a), the elevated Ce/Nb ratios of the entire suite compared to values between 1.8 and 3 for MORB and E-MORB. However, there is no clear trace element difference between the older and younger age groups of volcanics.

The similarity in the trace element geochemistry between the two volcanic suites is emphasized in Figure 7b. The entire sample suites show a general coherent differentiation trend in a Zr/Y versus Zr diagram (Fig. 7b). The Ce/Y ratio in Figure 7c is used as a proxy for REE fractionation. The relatively large range in Ce/Y indicates that either the entire suite has undergone variable fractionation involving some minor phases or that there have been different degrees of partial melting in the source. We rule out the possibility of greater fractional crystallization being the dominant process because of coherence of diagrams showing Zr/Y, Ce/Nb or Ce/Y versus Zr. Therefore, it is more likely that the LREE/HREE fractionation is caused by partial melting processes in the mantle, possibly resulting from variations in heat or water in the source or variable amounts of decompression.

4. Discussion

4.1 Nature and age of Crimean volcanism

Our $^{40}Ar/^{39}Ar$ ages define two age groups: an older age group (middle-late Jurassic ages, ~172-158 Ma) and a younger age group (late Jurassic-early Cretaceous, ~151-142) (Fig. 5). The older group comes from the Bodrak/Simferopol area, whereas the younger group comes from the Karadag volcanic edifice on the southeastern shore of the island.

Magmatic rocks from both age groups belong to similar magmatic complexes. The magmatics of the older group (Simferopol area) are present as plutonic bodies, sills and feeder dykes within the pre-upper Jurassic sedimentary units and as lava flows. Magmatic rocks from the younger group (Karadag) are present within an isolated volcanic complex, and have not been seen to interfinger with the Triassic-Jurassic stratigraphy. From the major and trace element analysis, however, we cannot make a clear distinction between the younger and older age groups (Figs. 6 and 7). Therefore, we conclude that volcanics of both age groups result from the same geological processes.

The geochemistry is in line with a setting above a subduction zone, and the results lead us to suggest that the sampled magmatic rocks are relics of a volcanic arc.

The middle Jurassic ages for the Crimean volcanics in the Bodrak area are in agreement with proposed ages from earlier studies (Spiridonov et al., 1990a; Spiridonov et al., 1990b). The latest Jurassic to earliest Cretaceous ages (151-142 Ma) obtained for the Karadag volcanics, however, are in conflict with ages obtained from biostratigraphic dating. Further, no remnants of volcanics or ashes have been found intercalating with time-equivalent, uppermost Jurassic platform carbonates.

Muratov (1960) and Voznesensky et al. (1998) reported that the lower part of the Karadag volcanic sequence yields Bajocian (~176.6-167.7 Ma) fauna, and that the volcanic complex is overlain by Bathonian to lower Callovian clays (~167.7-161.2 Ma) (Ogg, 2004), which casts doubt on the latest Jurassic to earliest Cretaceous ages. Alternatively, if the ages of the sediments based on biostratigraphy are correct, the contact between the overlying Jurassic rocks and the Karadag volcanic complex must be a thrust. This is possible given the tectonized nature of the Karadag complex: the sequence is heavily folded and faulted (Fig. 3b and c) (Voznesensky et al., 1998). The upper Jurassic platform carbonates are much less deformed than the Karadag volcanic complex. Possibly, the deformation of the Karadag complex is related to its location of Karadag at the Black Sea coast.

Assuming that our obtained ages are correct, the fact that no remnants of latest Jurassic to earliest Cretaceous volcanism can be traced in the upper Jurassic platform carbonates may have three possible explanations: it could imply that either a) the upper Jurassic carbonates or b) the Karadag volcanic complex have an allochthonous origin or that c) the volcanics erupted in intra-Berriasian times, the Berriasian on Crimea being marked by an unconformity.

The first of these possibilities, an allochthonous origin of the carbonate platform – emplaced during the Berriasian – has been proposed by Mileyev et al. (1996). This seems very unlikely, however, because it would imply that exactly the time-interval that is covered by the carbonate platform is missing in the entire Crimean stratigraphy, except for the Kimmeridgian comglomerates (see *Geology of Crimea* section). Furthermore, Mileyev et al. (1996) propose a displacement of the carbonate platform of only 15-20 km,

which would still not explain the absence of volcanics in the carbonate platform. If the carbonate platform would have been transported further than the distance proposed by Mileyev et al. (1996), the most likely origin of an allochthonous carbonate platform would be from the Turkish Pontides. In the Turkish Pontides however, the carbonate platform covers also the Callovian interval (Altıner et al., 1991; Rojay and Altiner, 1998), in contrast to Crimea. It would therefore be unlikely that the entire carbonate platform, except for the Callovian part, would have been transported from the Pontides.

The second possibility is an allochtonous origin of the Karadag aged volcanic complex, but this only transfers the problem of the presence of uppermost Jurassic to lowermost Cretaceous volcanics to other areas, because in the Greater Caucasus and the Pontides there are also no remnants of volcanism present in carbonates of this age.

The third option, the eruption of the volcanics in the middle Berriasian, instead of the latest Jurassic-earliest Cretaceous, is in agreement with our obtained ages (Fig. 5). This time interval is marked by uplift and erosion on Crimea (Mileyev et al., 1995; Nikishin et al., 2001), followed by conglomerate deposition in the late Berriasian. Volcanic activity would then occur during emersion and erosion of the carbonate platform. The third option would be a mechanism to reconcile the ages of the volcanics with the regional biostratigraphic constraints, although we cannot ignore the large difference between the stratigraphic and isotopic ages and the fact that no volcanic relics can be found in the Berriasian stratigraphy.

The conflict between the biostratigraphic and isotopic ages needs to be resolved by further investigations of the Karadag volcanic complex. Re-analysis of the biostratigraphy may shed conclusive light on this matter. The good agreement between the isotopic and biostratigraphic age groups in the Simferopol area (older age group), leads us to conclude that in the middle Jurassic Crimea was placed in an overriding plate of a subduction zone that lies to the south of Crimea, because there is no evidence for a suture north of the peninsula.

In the early Cretaceous, Crimea was covered with rift-related sediments. The rift sediments are likely associated with the opening of the Black Sea basins, as a result of back-arc spreading. Crimea was thus in an overriding plate position in the Jurassic (as

earlier proposed by Zonenshain and Le Pichon (1986)), as well as during the early Cretaceous and younger development of the Black Sea.

4.2 Implications for the Jurassic circum-Black Sea paleosubduction zone configuration

The $^{40}Ar/^{39}Ar$ isotopic dating of Crimean volcanics reveals an age range of ~172-142 Ma and our geochemical analyses suggest that volcanism is subduction-related. The latest Jurassic to earliest Cretaceous isotopic ages however, are in conflict with the biostratigraphy. Therefore, we conclude that middle Jurassic subduction took place below Crimea (Fig. 8a). If the latest Jurassic to earliest Cretaceous ages can be confirmed by future studies, we can conclude that subduction continued until the earliest Cretaceous and that the distance between Crimea and the subduction zone was more or less constant in the entire time span, as there is no major change from tholeiitic basalts to more evolved andesitic-rhyolites.

The presence of a volcanic arc places Crimea on the overriding plate of a subduction zone. Given the fact that Crimea overlies Scythian basement of the East European Platform (Saintot et al., 2007; Stephenson et al., 2004), subduction must have been directed northward (Fig. 8a). This contradicts reconstructions of Stampfli and Borel (2002) who prefer a southward Jurassic subduction zone between Crimea and the Pontides, with a polarity of subduction below the Pontides. For the southward subduction of the Küre ocean below the Pontides, as envisaged by Moix et al. (2008), we can now conclude that it must have been closed by 170 Ma, for since that time we can demonstrate northward subduction.

Northward subduction below Crimea from middle Jurassic to early Cretaceous times thus implies the presence of a northward directed subduction zone south of Crimea. There are two possible options for the location of an approximately east-west trending trench: 1) between Crimea, and the İstanbul and Sakarya zones and 2) south of the Pontides. Because the eastern Pontides also have a volcanic arc record in the middle Jurassic (Şen, 2007), the trench should be positioned south of the eastern Pontides, as well as south of the Greater Caucasus and Lesser Caucasus, because of the subduction-

related middle Jurassic volcanics in those areas. A recent study by Genç and Tüysüz (2010) shows evidence for subduction below the Sakarya Zone (western and central Pontides) in the middle Jurassic, therefore ruling out the possibility of the presence of a subduction zone between the Sakarya terrane and Crimea (Fig. 1). This option is also less favored, because the eastern Pontides were positioned in an overriding plate position. The configuration would then require a transform fault between the western and eastern Pontides, which seems to be precluded by the apparent continuity of the basement terranes from the western to the eastern Pontides.

It thus seems most likely that the Pontides as a whole were positioned in an overriding plate position in the Jurassic. An important implication of this inference, however, is that the volcanic arc in the western and central Pontide segment, as well as Crimea, is located ~500 km to the north of the subduction zone, when correcting for ~100-150 km of extension related to the opening of the Black Sea (Cloetingh et al., 2003; Shillington et al., 2008; Starostenko et al., 2004). Comparable estimates would be reached for the Transcaucasus and Caucasus segment. Although this distance is large, given general trench-arc distances on the order of 100-200 km, it is not exceptional. Arc-trench distances of 400 km (e.g. South American Andes) or even 600 km (Aleutian trench) (Gutscher et al., 2000) are generally attributed to flat-slab subduction (Brocher et al., 1994; Gutscher et al., 2000; van Hunen et al., 2002).

A fairly continuous trench south of the Pontides to at least as far east as the Caucasus region thus seems the most likely configuration in the middle Jurassic, and possibly until the earliest Cretaceous (Fig. 8a). In early Cretaceous times, this subduction zone likely started to retreat, with the Black Sea basin opening as back-arc basin (Fig. 8b).

5. Conclusion

This study shows that the sampled Crimean volcanics - previously assumed to be middle Jurassic in age - yield middle Jurassic to earliest Cretaceous $^{40}Ar/^{39}Ar$ ages (~172-142 Ma, i.e. ~Bajocian to Berriasian) (Fig 8a). The late Jurassic to earliest Cretaceous ages come from a single volcanic complex and are in conflict with the biostratigraphy, which requires further research. Our new geochemical data suggest that the volcanics

were formed in a subduction setting on the overriding plate, indicating a period of northward subduction below the Eurasian margin. The trench-arc distance derived from samples of all ages appears more or less constant, as there is no significant change from tholeiitic basalts to more evolved andesitic-rhyolites. After the Jurassic period characterized by arc-volcanism, the area is subject to (back-arc) rifting, with the opening the Black Sea basins (Fig. 8b) since the early Cretaceous. We propose that the subduction trench was located south of the Turkish Sakarya Zone and the Caucasus, as suggested by middle Jurassic arc-volcanics in those regions, placing them in the overriding plate. This would require flat-slab subduction, because the distance from Crimea to the trench, prior to Black Sea opening, is estimated at ~500 km.

Acknowledgements

The geochemistry data are part of the MSc thesis of BV, the research was carried out at VU University Amsterdam. We would like to thank Françoise Chalot-Prat for her help with inspection of the thin sections. Roel van Elzas is thanked for his help in the mineral-separation lab. The authors would like to thank a number of people for their help in the field and for discussion: Vladimir Bakhmutov, Sergei Bolotov, Tommy McCann, Françoise Chalot-Prat, Martijn Deenen, Wout Krijgsman, Yann Rolland, Oleg Rusakov and Stephen Vincent. The manuscript benefited from the comments of two anonymous reviewers. DJJvH acknowledges StatoilHydro for financial support (SPlates Model project). MJMM acknowledges the Netherlands Research Centre for Integrated Solid Earth Sciences (ISES) and the Netherlands Organization for Scientific Research (NWO) for financial support. The sampling campaigns in 2002 and 2004 were partly funded by the Middle East Basins Evolution (MEBE) program.

Figure caption

Figure 1

Map showing the most important tectonic blocks and sutures in a present-day geographical map. Carp= Carpathians, IAE= İzmir-Ankara-Erzincan suture, K= Kargı Massif, NAFZ= North Anatolian Fault Zone, Rh.= Rhodope, Sr= Srednogorie, TB= Thrace basin.

Figure 2

Early Kimmeridgian (~155 Ma) paleogeographic reconstruction based on Dercourt et al. (2000). A=Apulia; Adr=Adria; As=Asteroussia= BD=Bey Dağları; DM=Dalmatia; Dr= Drama; EP=eastern Pontides; ET=eastern Taurides; Fr=Friuli; G=Gavrovo; GCT=Greater Caucasus Through; GeZ= Getic Zone; Ks=Kırşehir Massif; Me=Menderes Massif; NTc= Northern Transcaucasus; P=Parnassos; Rh=Rhodopes; SAB= South Armenian Block, SCrT=South Crimean Through; Se=Severin; SP=Serbo-Pelagonian; Str= Strandja; TP=Tisza Plate; WP=western Pontides. White areas are areas without data.

Figure 3

a) Geological map of Crimea, based on Derenyuk et al. (1984) and Panek et al. (2009), with our sampling locations indicated.

b) Tilted pillow basalts from Karadag (top to the left; sample 04KAR1).

c) Verticalized columnar lava flow from Karadag (top to the left).

Figure 4

Figure showing the incremental heating $^{40}Ar/^{39}Ar$ spectra of 11 samples. The width of the bars/steps represents the 2σ analytical error. Weighed mean plateau ages are displayed. For all samples, also the K/Ca and inverse isochron diagrams, with their ages and inverse isochron intercept (iii) are shown.

Figure 5

Figure showing the $^{40}Ar/^{39}Ar$ ages. There are clearly two age groups that are also geographically spread over two areas: the Karadag volcanic edifice and the Bodrak/Simferopol area. Hett.=Hettangian; Pliensb.=Pliensbachian; Aalen.=Aalenian; Baj.=Bajocian; Bat.=Bathonian; Call.=Callovian; Oxford.=Oxordian; Kimm.=Kimmeridgian; Tithon.=Tithonian; Berrias.=Berriasian; Valangin.=Valanginian; Haut.=Hauterivian; Barr.=Barremian.

Figure 6

Plot of magmatic rocks (subdivided in four series, as indicated in the figure) in TAS classification diagram that displays (Na_2O + K_2O) versus SiO_2 (Le Maître et al., 1989). Area above (below) the dotted line indicates the alkaline (subalkaline or tholeiitic) field after Irvine and Baragar (1971).

Figure 7

a) Ce/Nb ratio versus Zr diagram of all data. The high Ce/Nb ratio is an indication for subduction related volcanism.

b) Zr/Y ratio versus Zr diagram of all data. The high Zr/Y ratio is an indication for subduction related volcanism.

c) Ce/Y ratio versus Zr diagram of all data. Note that the samples of the younger age group have on average a higher Ce/Y ratio, indicating so a greater LREE/HREE fractionation.

Figure 8

Proposed paleo-subduction zone configuration for the circum-Black Sea region in a) the middle Jurassic (~165 Ma) and b) the early Cretaceous (~120 Ma). Abbreviations as for Figure 2.

Supplementary data

Table with all individual incremental heating steps for all samples used for $^{40}Ar/^{39}Ar$ dating. Missing steps were not interpreted, because the amount of released argon was too high, leading to peak suppression. $^{40}Ar_r$: radiogenic amount of $^{40}A_r$ released in incremental heating step; $^{39}Ar_{(k)}$ (%): percentage of $^{39}Ar_{(k)}$ released in incremental heating step; 1s: 1σ; 2s: 2σ. Third column indicates the steps that are used for age calculation.

References

Adamia, S.A. et al., 1981. Tectonics of the Caucasus and adjoining regions: implications for the evolution of the Tethys ocean. Journal of Structural Geology 3(4): 437-447.

Altıner, D., Koçyiğit, A., Farinacci, A., Nicosia, U. and Conti, M.A., 1991. Jurassic-lower Cretaceous stratigraphy and paleogeographic evolution of the southern part of north-western Anatolia (Turkey). Geologica Romana 27: 13-80.

Arkad'ev, V.V., Fedorova, A.A., Savel'eva, Y.N. and Tesakova, E.M., 2006. Biostratigraphy of Jurassic–Cretaceous Boundary Sediments in the Eastern Crimea. Stratigraphy and Geological Correlation 14(3): 302-330.

Arkad'ev, V.V. and Rogov, M.A., 2006. New Data on Upper Kimmeridgian–Tithonian Biostratigraphy and Ammonites of the Eastern Crimea. Stratigraphy and Geological Correlation 14(2): 185-199.

Banks, C.J. and Robinson, A.G., 1997. Mesozoic strike-slip back-arc basins of the western Black Sea region. In: A.G. Robinson (Editor), Regional and petroleum geology of the Black Sea and surrounding regions. AAPG Memoir, pp. 53-62.

Baraboshkin, E., 2003. Early Cretaceous development of the Mountain Crimea. Annual, Geology and Geophysics 46(1): 25-30.

Barrier, E. and Vrielynck, B., 2008. Paleotectonic maps of the Middle East. Middle East Basins Evolution Programme, CCGM-CGMW, Paris.

Besse, J. and Courtillot, V., 2002. Apparent and true polar wander and the geometry of the geomagnetic field in the last 200 million years. Journal of Geophysical Research 107(B11): doi:10.1029/2000JB000050.

Bozkurt, E., Holdsworth, B.K. and Koçyiğit, A., 1997. Implications of Jurassic chert identified in the Tokat Complex. Geological Magazine 134: 91-97.

Bozkurt, E., Winchester, J.A., Yiğitbaş, E. and Ottley, C.J., 2008. Proterozoic ophiolites and mafic-ultramafic complexes marginal to the İstanbul Block: An exotic terrane of Avalonian affinity in NW Turkey. Tectonophysics 461: 240-251.

Brocher, T.M., Fuis, G.S., Fisher, M.A., Plafker, G. and Moses, M.J., 1994. Mapping the megathrust beneath the northern Gulf of Alaska using wide-angle seismic data. Journal of Geophysical Research 99(B6): 11,663-11,685.

Çelik, Ö.F., Delaloyle, M.F. and Feraud, G., 2006. Precise ^{40}Ar–^{39}Ar ages from the metamorphic sole rocks of the Tauride Belt Ophiolites, southern Turkey: implications for the rapid cooling history. Geological Magazine 143: 213-227.

Chen, F., Siebel, W., Satir, M., Terzioglu, M.N. and Saka, K., 2002. Geochronology of the Karadere basement (NW Turkey) and implications for the geological evolution of the Istanbul zone. International Journal of Earth Sciences 91: 469-481.

Cloetingh, S., Spadini, G., Van Wees, J.D. and Beekman, F., 2003. Thermo-mechanical modelling of Black Sea Basin (de)formation. Sedimentary Geology 156: 169-184.

Dercourt, J. et al., 2000. Peri-Tethys Palaeogeographical Atlas. Gauthier Villars.

Dercourt, J., Ricou, L.E. and Vrielynck, B. (Editors), 1993. Atlas Tethys Paleoenvironmental Maps, Beicip-Franlab, Town.

Derenyuk, N.E., Vanina, M.V., Gerasimov, M.Y. and Pirovarov, S.V., 1984. Geological map of the Crimea. Geological Ministry of Ukraine (In Russian), Kiev.

Dokuz, A., Tanyolu, E. and Genç, S., 2006. A mantle- and a lower crust-derived bimodal suite in the Yusufeli (Artvin) area, NE Turkey: trace element and REE evidence for subduction-related rift origin of Early Jurassic Demirkent intrusive complex. International Journal of Earth Sciences 95: 370-394.

Elmas, A. and Yiğitbaş, E., 2001. Ophiolitie emplacement by strike-slip tectonics between the Pontide Zone and the Sakarya Zone in northwestern Anatolia, Turkey. International Journal of Earth Sciences 90: 257-269.

Favre, P. and Stampfli, G.M., 1992. From rifting to passive margin: the examples of the Red Sea, Central Atlantic and Alpine Tethys. Tectonophysics 215: 69-97.

Finetti, J.K., Price, G.D., Hart, M.B. and Leng, M.J., 1988. Geophysical study of the Black Sea. Bollettino di Geofisica Teorica ed Applicata XXX(117-118): 197-324.

Fisher, J.K., Price, G.D., Hart, M.B. and Leng, M.J., 2005. Stable isotope analysis of the Cenomanian-Turonian (Late Cretaceous) oceanic anoxic event in the Crimea. Cretaceous Research 26(6): 853-863.

Fleck, R.J., Sutter, J.F. and Elliot, D.H., 1977. Interpretation of discordant $^{40}Ar/^{39}Ar$ age-spectra of Mesozoic tholeootes from Antarctica Geochimica et Cosmochimica Acta 41: 15-32.

Genç, Ş.C. and Tüysüz, O., 2010. Tectonic setting of the Jurassic bimodal magmatism in the Sakarya Zone (Central and Western Pontides), Northern Turkey: A geochemical and isotopic approach. Lithos 118: 95-111, doi: 10.1016/j.lithos.2010.03.017.

Genç, S.C. and Yilmaz, Y., 1995. Evolution of the Triassic continental margin, northwest Anatolia. Tectonophysics 243: 193-207.

Gerasimov, M.E., 1994. Deep structure and Evolution of the Southern Margin of the East-European Platform According to Seismostratigraphical Data, and Connection with Oil and Gas Potential, VNIGRI, Moscow.

Gorbatchev, R. and Bogdanova, S., 1993. Frontiers in the Baltic Shield. Precambrian Research 64: 3-21.

Görür, N., 1997. Cretaceous Syn- to Postrift Sedimentation on the Southern Continental Margin of the Western Black Sea Basin. In: A.G. Robinson (Editor), Regional and petroleum geology of the Black Sea and surrounding region. AAPG Memoir, pp. 227-240.

Gutscher, M.-A., Spakman, W., Bijwaard, H. and Engdahl, E.R., 2000. Geodynamics of flat subduction: Seismicity and tomographic constraints from the Andean margin. Tectonics 19(5): 814-833.

Hein, C., 2005. Das Konglomerat der mittel- bis spätjurassischen Taphanskaya Formation im Demerdji Gebirge (Südkrim/Ukraine). MSc Thesis, Universitat Bonn, Bonn.

Hippolyte, J.-C., Müller, C., Kaymakci, N. and Sangu, E., 2010. Nannoplankton dating in the Black Sea inverted margin of Central Pontides (Turkey) reveals two episodes of rifting. In: M. Sosson, N. Kaymakci, R.A. Stephenson, V. Starostenko and F. Bergerat (Editors), Sedimentary basin tectonics from the Black Sea and Caucasus to the Arabian Platform. Geological Society of London, London.

Hudson, S.M. et al., 2008. Stratigraphy and geochemical characterization of the Oligocene-Miocene Maikop series: Implications for the paleogeography of Eastern Azerbaijan. Tectonophysics 451: 40-55.

Irvine, T.N. and Baragar, W.R.A., 1971. Chemical differententioation of the Earth: the relationship between mantle, continental crust and oceanic crust. Canadian Journal of Earth Sciences 8: 523-548.

Kaymakci, N., Özçelik, Y., White, S.H. and Van Dijk, P.M., 2009. Tectono-stratigraphy of the Çankırı Basin: late Cretaceous to early Miocene evolution of the

Neotethyan suture zone in Turkey. In: D.J.J. Van Hinsbergen, M.A. Edwards and R. Govers (Editors), Collision and Collapse at the Africa-Arabia-Eurasia subduction zone. Special Publication. Geological Society of London, London, pp. 67-106.

Kazmin, V.G. et al. (Editors), 1987. Volcanic belt-indicators of the Mesozoic-Cenozoic sctive outskirts of Eurasia. History of the Tethys Ocean. Academy of Sciences of the USSR, P.P. Shirshov Institute of Oceanology, Moscow, 58-74 (In Russian) pp.

Kent, D.V. and May, S.R., 1987. Polar Wander and Paleomagnetic Reference Pole Controversies. Reviews of Geophysics 25(5): 961-970.

Khain, V.Y., 1984. Regionalnaya geotektonika. Alpiysko–Sredizemnomorskiy poyas. (Regional geotectonics. The Alpine–Mediterranean Belt). Nedra, Moscow, 344 pp.

Koppers, A.A.P., 2002. ArArCalc software for $^{40}Ar/^{39}Ar$ age calculations. Computational Geosciences 28: 605-619.

Koronovsky, N.V. and Mileyev, V.S., 1974. O sootnoshenii otlojenii Tavricheskoi serii i eskiordinkoi svity v doline r. Bodrak (Gornnii Krim) (About the relationships of Tauric series and Eskiorda suite in the Bodrak river valley (Mountain Crimea)). Vestnik Moskovskogo Universiteta Geologiya 1: 80-87.

Krajewski, M. and Olszewska, B., 2006. New data about microfacies and stratigraphy of the Late Jurassic Aj-Petri carbonate buildup (SW Crimea Mountains, S Ukraine). Neues Jahrbuch für Geologie und Paläontologie, Monatshefte 5: 298-312.

Kriachtchevskaia, O., Stovba, S. and Stephenson, R., 2010. Cretaceous-Cenozoic evolution of the Odessa Shelf and Azov Sea from seismic data and 1-D modelling In: M. Sosson, N. Kaymakci, R.A. Stephenson, V. Starostenko and F. Bergerat (Editors), Sedimentary basin tectonics from the Black Sea and Caucasus to the Arabian Platform. Geological Society of London, London.

Kruglov, S.S. and Tsypko, A.K., 1988. Tectonics of the Ukraine. Nedra, Moscow, 1-254 (In Russian) pp.

Lalomov, A., 2007. Reconstruction of paleohydrodynamic conditions during the formation of Upper Jurassic conglomerates of the Crimean Peninsula. Lithology and Mineral Resources 42(3): 268-280.

Latyshev, A.V. and Panov, D.I., 2008. Jurassic magmatic bodies of Mountainous Crimea in the Bodrak River catchment (Southwestern Crimea). Moscow University Bulletin 63(2): 70-78.

Le Maître, R.W. et al., 1989. A Classification of Igneous Rocks and Glossary of Terms. Blackwell, Oxford, 193 pp.

Letavin, A.I., 1980. Basement of the Young Platform of the Southern USSR, Nauka, Moscow.

Lordkipanidze, M.B., Meliksetian, B. and Djarbashian, R. (Editors), 1989. Mesozoic-Cenozoic Magmatic Evolution of the Pontian-Crimean-Caucasian Region. IGCP project n°198: Evolution of the northern margin of Tethys, 154 (II). Mémoire de la Société Géologique de France, Paris, Nouvelle Série, Paris, 103-124 pp.

Mazarovich, O.A. and Mileev, V.S., 1989. Geological Structure of the Kacha Upland of the Mountain Crimea. Stratigraphy of the Mesozoic., Moscow, pp. 1-168 (In Russian).

McCann, T., Chalot-Prat, F. and Saintot, A., 2010. The Early Mesozoic evolution of the Western Greater Caucasus (Russia): Triassic-Jurassic sedimentary & magmatic history. In: M. Sosson, N. Kaymakcı, R. Stephenson, F. Bergerat and V. Starostenko (Editors), Sedimentary basin tectonics from the Black Sea and Caucasus to the Arabian Platform. Geolgical Society of London, London.

Milanovsky, E.E., 1991. Geology of the USSR. Part 3, Moscow University Press, Moscow.

Mileyev, V.S., Baraboshkin, E.Y., Nikitin, M.Y., Rozanov, S.B. and Shalimov, I.V., 1996. Evidence that the Upper Jurassic deposits of the Crimean Mountains are allochtons. Transactions (Doklady) of the Russian Academy of Sciences, Earth Science Sections 342(4): 121-124.

Mileyev, V.S., Rozanov, S.B., Baraboshkin, E.Y., Nikitin, M.Y. and Shalimov, I.V., 1995. The position of the Upper Jurassic deposits in the structure of the Mountain Crimea. Byulleten Moskovskogo Obshestva Ispytatelei Prirody, Geologia 70(1): 22-31 (In Russian).

Mileyev, V.S., Rozanov, S.B., Baraboshkin, E.Y. and Shalimov, I.V. (Editors), 1997. The tectonic structure and evolution of the Mountain Crimea. Geological study of Crimea. Geological Faculty MSU Publishers (In Russian), Moscow.

Moix, P. et al., 2008. A New Classification of the Turkish Terranes and Sutures and its Implications for the Paleotectonic History of the Region. Tectonophysics 451: 7-39.

Muratov, M.V., 1960. Kratkii ocherk geologicheskogo stroeniya Krymskogo poluostrova (Concise Review of the Geologic Structure of the Crimean Peninsula). Gosgeoltekhizdat, Moscow.

Muratov, M.V. (Editor), 1969. Geology of the USSR. Volume VIII: Crimea. Part 1: Geology. Nedra, Moscow, 1-576 (In Russian) pp.

Muratov, M.V., Arkhipov, I.V. and Uspenskaya, Y.A., 1984. Structural evolution of the Crimean mountains and comparison with the Western Caucasus and the Eastern Balkan ranges.

Nikishin, A.M. et al., 2008. The Cretaceous history of the Bakhchisaray area, southern Crimea (Ukraine). Bulletin de l'Institut royal des Sciences naturelles de Belgique, Sciences de la Terre 78: 75-85.

Nikishin, A.M. et al., 1998. Scythian Platform, Caucasus and Black Sea region: Mesozoic-Cenozoic tectonic history and dynamics. In: S. Crasquin-Soleau and E. Barrier (Editors), Peri-Tethys Memoir 3: Stratigraphy and Evolution of Peri-Tethyan Platforms. Mémoires Muséum national d'Histoire naturelle, Paris.

Nikishin, A.M., Korotaev, M.V., Ershov, A.V. and Brunet, M.-F., 2003. The Black Sea basin: tectonic history and Neogene-Quaternary rapid subsidence modelling. Sedimentary Geology 156: 149-168.

Nikishin, A.M. et al., 2001. Mesozoic and Cainozoic evolution of the Scythian Platform-Black Sea-Caucasus domain. In: P.A. Ziegler, W. Cavazza, A.H.F. Robertson and S. Crasquin-Soleau (Editors), Peri-Tethys Memoir 6: Peri-Tethyan Rift/Wrench Basins and Passive Margins. Mémoires Muséum national d'Histoire naturelle, Paris, pp. 295-346.

Nikishin, A.M. et al., 1996. Late Precambrian to Triassic history of the East European Craton: dynamics of sedimentary basin evolution. Tectonophysics 268: 23-63.

Ogg, J.G., 2004. The Jurassic Period. In: F.M. Gradstein, J.G. Ogg and A.G. Smith (Editors), A Geologic Time Scale 2004. Cambridge University Press, Cambridge, pp. 307-343.

Okay, A.I. et al., 2008. Defining the southern margin of Avalonia in the Pontides: Geochronological data from the Late Proterozoic and Ordovician granitoids from NW Turkey. Tectonophysics 461(1-4): 252-264.

Okay, A.I. and Göncüoğlu, C., 2004. The Karakaya complex: A review of data and concepts. Turkish Journal of Earth Sciences 13(2): 77-95.

Okay, A.I. and Monié, P., 1997. Early Mesozoic subduction in the Eastern Mediterranean: Evidence from Triassic eclogite in northwest Turkey. Geology 25(7): 595-598.

Okay, A.I., Monod, O. and Monie, P., 2002. Triassic blueschists and eclogites from northwest Turkey: vestiges of the Paleo-Tethyan subduction. Lithos 64(3-4): 155-178.

Okay, A.I. and Şahintürk, Ö., 1997. Geology of the Eastern Pontides. In: A.G. Robinson (Editor), Regional and petroleum geology of the Black Sea and surrounding region. AAPG Memoir, pp. 291-311.

Okay, A.I. et al., 1996. Paleo- and Neo-Tethyan events in northwestern Turkey: geologic and geochronologic constraints. In: A. Yin and T.M. Harrison (Editors), The tectonic evolution of Asia. Cambridge University Press, Cambridge, pp. 420-441.

Okay, A.I., Satır, M., Tüysüz, O., Akyüz, S. and Chen, F., 2001a. The tectonics of the Strandja Massif: late-Variscan and mid-Mesozoic deformation and metamorphism in the northern Aegean. International Journal of Earth Sciences 90: 217-233.

Okay, A.I., Şengör, A.M.C. and Görür, N., 1994. Kinematic history of the opening of the Black Sea and its effect on the surrounding regions. Geology 22: 267-270.

Okay, A.I., Tansel, I. and Tüysüz, O., 2001b. Obduction, subduction and collision as reflected in the Upper Cretaceous-Lower Eocene sedimentary record of western Turkey. Geological Magazine 138(2): 117-142.

Okay, A.I. et al., 2006. Cretaceous and Triassic subduction-accretion, HP/LT metamorphism and continental growth in the Central Pontides, Turkey. Geological Society of America Bulletin 118: 1247-1269.

Page, F., Wirth, K.R., Dobrovolskaya, T.I. and Thole, J.T., 1998. Subduction-related mid-Jurassic magmatism of the Crimean Mountains, Annual Meeting of the Geological Society of America, Toronto, Ontario, Abstracts with Programs, v. 30, p. 378.

Panek, T., Danisik, M., Hradecky, J. and Frisch, W., 2009. Morpho-tectonic evolution of the Crimean mountains (Ukraine) as constrained by apatite fission track data. Terra Nova 21(4): 271-278.

Pickett, E. and Robertson, A.H.F., 2004. Significance of the Volcanogenic Nilufer Unit and Related Components of the Triassic Karakaya Complex for Tethyan Subduction/Accretion Processes in NW Turkey. Turkish Journal of Earth Sciences 13: 97-143.

Popadyuk, I.V. and Smirnov, S.Y., 1991. The problem of the structure of the Crimean Mountain Region: Traditional ideas and reality. Geotectonics 25(6): 489-497.

Popadyuk, I.V. and Smirnov, S.Y., 1996. Crimean orogen, a nappe interpretation. In: P.A. Ziegler and F. Horvath (Editors), Peri-Tethys Memoir 2: Structure and

prospects of Alpine basins and forelands. Mémoires du Museum national d'Histoire naturelle, Paris, pp. 403-425.

Rice, S.P., Robertson, A.H.F. and Ustaömer, T., 2006. Late-Cretaceous- Early Cenozoic tectonic evolution of the Eurasian active margin in the Central and Eastern Pontides, northern Turkey. In: A.H.F. Robertson and D. Mountrakis (Editors), Tectonic Development of the Eastern Mediterranean Region The Geological Society of London, London, pp. 413-445.

Robertson, A.H.F. and Dixon, J.E., 1984. Introduction: aspects of the geological evolution of the Eastern Mediterranean. In: J.E. Dixon and A.H.F. Robertson (Editors), The geological evolution of the Eastern Mediterranean. Geological Society Special Publications, London, pp. 1-74.

Robertson, A.H.F. and Üstaömer, T., 2004. Tectonic evolution of the Intra-Pontide suture zone in the Armutlu Peninsula, NW Turkey. Tectonophysics 381: 175-209.

Robertson, A.H.F. et al., 2004. Testing models of Late Palaeozoic-Early Mesozoic orogeny in Western Turkey: support for an evolving open-Tethys model. Journal of the Geological Society, London 161: 501-511.

Robinson, A., Spadini, G., Cloetingh, S. and Rudat, J., 1995. Stratigraphic evolution of the Black Sea: inferences from basin modelling. Marine and Petroleum Geology 12(8): 821-835.

Robinson, A.G. and Kerusov, E., 1997. Stratigraphic and Structural Development of the Gulf of Odessa, Ukrainian Black Sea: Implications for Petroleum Exploration. In: A.G. Robinson (Editor), Regional and petroleum geology of the Black Sea and surrounding region. AAPG Memoir 68, pp. 369-380.

Robinson, A.G., Rudat, J.H., Banks, C.J. and Wiles, L.F., 1996. Petroleum geology of the Black Sea. Marine and Petroleum Geology 13(2): 195-223.

Rojay, B. and Altiner, D., 1998. Middle Jurassic-lower Cretaceous biostratigraphy in the Central Pontides (Turkey): remarks on paleogeography and tectonic evolution. Rivista Italiana di Paleontologia e Stratigrafia 104(2): 167-179.

Saintot, A. et al. (Editors), 2006a. The Mesozoic-Cenozoic tectonic evolution of the Greater Caucasus. European Lithosphere Dynamics. Geological Society London, London, 277-289 pp.

Saintot, A. et al., 2006b. The evolution of the southern margin of eastern Europe (Eastern European and Scythian platforms) from the latest Precambrian-Early Palaeozoic to the Early Cretaceous. In: D. Gee and S. R.A. (Editors), European Lithosphere Dynamics. Memoir. The Geological Society of London, London, pp. 481-505.

Saintot, A., Stephenson, R.A. and Chalot-Prat, F., 2007. The position of Crimea and Greater Caucasus along the active margin of Eurasia (from early Jurassic to present), Abstract Volume, International symposium on the Middle east Basins Evolution, Paris, December 4-5, p.c.69.

Şen, C., 2007. Jurassic volcanism in the Eastern Pontides: is it rift related or subduction related? Turkish Journal of Earth Sciences 16: 523-539.

Şengör, A.M.C. and Yilmaz, Y., 1981. Tethyan evolution of Turkey: A plate tectonic approach. Tectonophysics 75(3-4): 181-241.

Shillington, D.J. et al., 2008. Cenozoic evolution of the eastern Black Sea: A test of depth-dependent stretching models. Earth and Planetary Science Letters 265: 360-378.

Sosson, M. et al., In press. Subduction, obduction and collision in the Lesser Caucasus (Armenia, Azerbaijan, Georgia), new insights. In: M. Sosson, N. Kaymakci, R.A. Stephenson, F. Bergerat and V. Starostenko (Editors), Sedimentary basin tectonics from the Black Sea and Caucasus to the Arabian Platform. Geological Society of London, London.

Spiridonov, E.M., Fedorov, T.O. and Ryakhovskii, V.M., 1990a. Magmatic rocks of the Mountainous Crimea (1). Bulletin Moskovskogo Obshestva Ispytalelei Prirody, otd. geol. 65(4): 119-134.

Spiridonov, E.M., Fedorov, T.O. and Ryakhovskii, V.M., 1990b. Magmatic Rocks of the Mountainous Crimea (2). Bulletin Moskovskogo Obshestva Ispytalelei Prirody, otd. geol. 65(6): 102-112.

Stampfli, G.M. and Borel, G.D., 2002. A plate tectonic model for the Paleozoic and Mesozoic constrained by dynamic plate boundaries and restored synthetic oceanic isochrons. Earth and Planetary Science Letters 196(1-2): 17-33.

Stampfli, G.M. and Borel, G.D., 2004. The TRANSMED transects in space and time: Constraints on the paleotectonic evolution of the Mediterranean domain. In: W. Cavazza, F. Roure, W. Spakman, G.M. Stampfli and P. Ziegler (Editors), The TRANSMED Atlas: the Mediterranean Region from Crust to Mantle. Springer Verlag, Berlin, pp. 53-76.

Stampfli, G.M. and Kozur, H.W., 2006. Europe from the Variscan to the Alpine cycles. In: D.G. Gee and R.A. Stephenson (Editors), European lithosphere dynamics. Memoir of the Geological Society, London, pp. 57-82.

Starostenko, V. et al., 2004. Topography of the crust–mantle boundary beneath the Black Sea Basin. Tectonophysics 381: 211-233.

Steiger, R.H. and Jäger, E., 1977. Subcommission on geochemistry: convention on the use of decay constants in geo- and cosmochronology. Earth and Planetary Science Letters 36(359-362).

Stephenson, R.A. et al., 2004. Transect VIII: Eastern European Craton to Arabian Craton (Red Star to Red Sea). In: W. Cavazza, F.M. Roure, W. Spakman, G.M. Stampfli and P.A. Ziegler (Editors), The TRANSMED Atlas – The Mediterranean region from crust to mantle. Springer Verlag, Berlin Heidelberg.

Stolyarov, A.S. and Ivleva, E.I., 2006. Lower Miocene sediments of the Maikop Group in the Central Eastern Paratethys. Lithology and Mineral Resources 41(1): 54-72.

Sun, S.S. and McDonough, W.F., 1989. Chemical and isotopic systematics of oceanic basalts: implications for mantle composition and processes. In: A.D. DSaudners and M.J. Norry (Editors), Magmatism in Ocean Basins. Geological Society Special Publications, London, pp. 313-345.

Sysolin, A.I. and Pravikova, N.V., 2008. Subvolcanic Bodies of the Bodrak Complex in the Southwestern Crimea: Structure, Composition, and Formation Conditions. Moscow University Bulletin 63(2): 79-85.

Topuz, G. and Altherr, R., 2004. Pervasive rehydration of granulites during exhumation – an example from the Pulur complex, Eastern Pontides, Turkey. Mineralogy and Petrology 81: 165-185.

Topuz, G. et al., 2004. Aluminous granulites from the Pulur complex, NE Turkey: a case of partial melting, efficient melt extraction and crystallisation. Lithos 72: 183-207.

Topuz, G., Altherr, R., Schwarz, W.H., Dokuz, A. and Meyer, H.-P., 2007. Variscan amphibolite-facies rocks from the Kurtoglu metamorphic complex (Gümüshane area, Eastern Pontides, Turkey). International Journal of Earth Sciences 96: 861-873.

Torsvik, T.H., Muller, R.D., Van der Voo, R., Steinberger, B. and Gaina, C., 2008. Global plate motion frames: toward a unified model. Reviews of Geophysics 46: RG3004, doi:10.1029/2007RG000227.

Tüysüz, O., 1999. Geology of the Cretaceous sedimentary basins of the Western Pontides. Geological Journal 34: 75-93.

Ustaömer, P.A., Mundil, R. and Renne, P.R., 2005. U/Pb and Pb/Pb zircon ages for arc-related intrusions of the Bolu Massif (W Pontides, NW Turkey): evidence for Late Precambrian (Cadomian) age. Terra Nova 17: 215-223.

Üstaömer, T. and Robertson, A.H.F., 1993. A Late Paleozoic-Early Mesozoic marginal basin along the active southern continental margin of Eurasia: evidence from the central Pontides (Turkey) and adjacent regions. Geological Journal 28: 219-238.

van Hunen, J., van den Berg, A.P. and Vlaar, N.J., 2002. On the role of subducting oceanic plateaus in the development of shallow flat subduction. Tectonophysics 352: 317-333.

Vincent, S.J. et al., 2005. Insights from the Talysh of Azerbaijan into the Paleogene evolution of the South Caspian region. GSA Bulletin 117(11/12): 1513-1533; doi: 10.1130/B25690.1.

Voznesensky, A.I., Knipper, A.L., Perfiliev, A.S., Uspenskaya, A.E. and Areshin, A.V., 1998. Middle-Late Jurassic history of the Eastern Crimean Mts. Terrane. Geotektonika 1: 27-44.

Wijbrans, J.R., Pringle, M.S., Koppers, A.A.P. and Scheveers, R., 1995. Argon geochronology of small samples using the Vulkaan argon laserprobe. Proc. van de Koninklijke Nederlandse Academie van Wetenschappen 98(Ser. B): 185-218.

Yalınız, K.M., Göncüoglu, M.C. and Özkan-Altıner, S., 2000. Formation and emplacement ages of the SSZ-type Neotethyan ophiolites in Central Anatolia, Turkey: palaeotectonic implications. Geological Journal 35: 53-68.

Yılmaz, C. and Kandemir, R., 2006. Sedimentary records of the extensional tectonic regime with temporal cessation: Gumushane Mesozoic Basin (NE Turkey) Geologica Carpathica 57(1): 3-13.

Yılmaz, C., Şen, C. and Özgür, A.S., 2003. Sedimentological, paleontological and volcanic records of the earliest volcanic activity in the Eastern Pontide Cretaceous volcanic arc (NE Turkey). Geologica Carpathica 54(6): 377-384.

Zonenshain, L.P., Kuzmin, M.I. and Napatov, L.M. (Editors), 1990. Geology of the USSR: a Plate-Tectonic Synthesis Geodunamics Series, 21. American Geophysical Union.

Zonenshain, L.P. and Le Pichon, X., 1986. Deep basins of the Black Sea and Caspian Sea as remnants of Mesozoic back-arc basins. Tectonophysics 123: 181-211.

Table 1. Mineralogy of the samples selected for $^{40}Ar/^{39}Ar$ dating, determined from microscope inspection.

KARS01	nuee ardente (rhyolite)	vitroclastic; white/green color; >25% pumiceous; fresh plagioclase, low amount however
04CRLEB	andesite	large fraction fresh hornblende; fresh biotite (large fraction, but less common than amphibole); porphyritic texture with interstitial calcite; pseudomorph glass?; pseudomorph augite; fresh plagioclase (common)
KA28b	trachyte	fresh plagioclase phenocrysts; porphyritic and microlithic texture; some plagioclase contains calcite
04KAR1	pillow lava (basaltic) andesite	porphyritic & finely microlithic texture with vesicles in the glass; augite (slightly pleochroic); very fresh plagioclase; vesicles probably filled with clay
IKUCH7	(trachy-) andesite	chlorite probably pseudomorph in glass; plagioclase is interfingered with a matrix of chlorite (pseudomorph); alkali-feldspar grains present (one twin); probaly phenocrysts of plagioclase; perhaps interstitial quartz; no ferromagnesium silicate
LBOD16	basalt	very fresh plagioclase; a lot of calcite in matrix, in patches; porphyritic and mirolithic texture; some augite present; maybe some olivine present
FET4G	andesitic lava with columnar joints	porphyritic and mirolithic texture; calcite is replacing the plagioclase; feldspar not very fresh, but twins are visible; phenocrysts of plagioclase; plagioclase microliths; microcrystalline quartz present in vesicles
CUKR3	alkali-syenite-monzonite	some fresh amphibole present; K-feldspar is more or less fresh; plagioclase; ironoxides; interstitial quartz; completely crystalline; probably an intrusion, because minerals had time to grow over each other; no glass.
KIZ41	andesitic lava	phenocrysts of brown amphibole (hornblende) with black rims formed by iron oxides; biotite; few phenocrysts of zoned plagioclase; porphyritic and microlithic texture; matrix (~90%) is essentially made of feldspar microcrystals, iron oxides and calcite.
TRU6FL	andesitic lava	almost completely crystalline rock, consists of 80% feldspar (orthose and plagioclase, sometimes zoned); remaining 20% twinned augites and iron oxides; porphyritic and microlithic texture

Table 2. Summary of $^{40}Ar/^{39}Ar$ results.

MSWD: mean square weighted deviates, N: number of steps included (excluded) in the plateau age, $^{39}Ar_k$ (%): percentage of $^{39}Ar_k$ released by plateau steps, $^{40}Ar_r$: radiogenic amount of $^{40}A_r$. Errors are given at 95% confidence level. Ages were calculated using the in-house developed ArArCalc software (Koppers, 2002). All $^{40}Ar/^{39}Ar$ ages were calculated using Steiger and Jäger (1977) decay constants at the 2 level and include the analytical error and error in irradiation parameter (J). Correction factors for neutron interference reactions are $2.7 \pm 0.03 \times 10^{-4}$ for $(^{36}Ar/^{37}Ar)Ca$, $6.99 \pm 0.13 \times 10^{-4}$ for $(^{39}Ar/^{37}Ar)Ca$ and $1.83 \pm 0.2 \times 10^{-2}$ for $(^{40}Ar/^{39}Ar)K$. Strikethrough plateau ages indicate error plateaus.

Irradiation	sample ID	sampling latitide (º)	sampling longitude (º)	Lab ID	Mineral	Fraction (mm)	J (+/- 0.4%)	Plateau age (Ma)	MSWD	N	39ArK (%) in plateau	40Arr (%)	K/Ca	Total fusion age (Ma)	Inverse isochron age (Ma)	Inverse isochron intercept
VU65-B2	*FET4G*	*44.915*	*34.176*	07MX363	plagioclase	200-250	0.0075000	No plateau	-	-	-	-	-	4134.9 ± 9.7	-	-
VU65-B3	*KA28b*	*44.913*	*35.205*	07MX364	plagioclase	200-250	0.0075540	151.0 ± 5.8	2.00	7 (5)	81.34	45.07	0.013 ± 0.002	201.3 ± 57.6	153.8 ± 11.6	290.2 ± 19.1
VU65-B4	*CUKR3*	*44.900*	*34.142*	07MX365	plagioclase	125-250	0.0075580	170.7 ± 5.2	3.53	19 (1)	99.96	31.73	0.062 ± 0.011	174.3 ± 4.4	162.9 ± 17.2	302.6 ± 15.5
VU65-B5	*LBOD16*	*44.785*	*33.992*	07MX366	plagioclase	200-250	0.0075630	158.3 ± 7.0	0.39	13 (5)	66.53	32.50	0.004/0.000	148.5 ± 9.6	158.1 ± 17.9	295.7 ± 15.5
VU65-B6	*04CRLEB*	*44.752*	*34.055*	07MX368	plagioclase	200-250	0.0075670	171.3 ± 2.6	1.53	15 (4)	70.85	55.33	0.027 ± 0.003	184.1 ± 3.5	169.9 ± 5.7	299.6 ± 13.3
VU65-B8	*IKUCH7*	*44.780*	*34.029*	07MX369	plagioclase	125-250	0.0075760	160.4 ± 2.0	2.42	21 (3)	81.41	68.28	0.039 ± 0.045	176.8 ± 6.4	159.2 ± 3.3	300.5 ±11.4
VU65-B9	*04KAR1*	*44.913*	*35.225*	07MX370	plagioclase	200-250	0.0075800	143.2 ± 2.9	0.45	16 (4)	70.56	64.38	0.007 ± 0.000	112.3 ± 3.3	145.3 ± 6.7	288.2 ± 22.2
VU65-B10	*KARS01*	*44.934*	*35.232*	07MX371	plagioclase	125-250	0.0075840	143.1 ± 1.8	2.49	10 (4)	49.18	92.25	0.063 ± 0.013	154.4 ± 1.7	139.9 ± 5.5	366.6 ± 110.6
VU65-B11	*KA28b*	*44.913*	*35.205*	07MX373	ground mass	250-500	0.0075880	152.0 ± 2.5	2.00	20 (13)	24.43	49.68	0.150 ± 0.007	162.8 ± 3.1	140.4 ± 7.9	319.4 ± 15.8
VU65-B12	*KA28b*	*44.913*	*35.205*	07MX374	ground mass	250-500	0.0075930	148.5 ± 1.8	0.59	19 (15)	16.91	66.37	0.248 ± 0.012	161.0 ± 2.3	142.8 ± 10.0	319.1 ± 40.7
Comb.	*KA28b*	*44.913*	*35.205*	Comb.	ground mass	250-500	-	148.4 ± 2.0	4.55	39 (23)	50.15	59.72	0.174 ± 0.023	161.3 ± 2.1	143.1 ± 2.4	315.8 ± 7.1
VU65-B14	*FET4G*	*44.915*	*34.176*	07MX375	ground mass	250-500	0.0076010	467.6 ± 58.1	0.29	15 (6)	45.24	5.32	0.290 ± 0.044	473.7 ± 42.2	458.4 ± 353.4	295.9 ± 19.9
VU52-B8	*KIZ41*	*44.822*	*34.053*	05MY313	biotite	250-500	0.0046470	168.0 ± 3.2	1.03	10 (4)	68.22	96.82	0.025 ± 0.001	162.5 ± 3.7	165.0 ± 7.8	516.1 ± 792.4
VU52-B4	*TRU6FL*	*44.788*	*33.996*	05MY027	ground mass	250-500	0.0046620	165.7 ± 1.3	0.54	17 (11)	61.59	70.34	0.077 ± 0.004	161.1 ± 1.2	166.3 ± 3.0	292.8 ± 13.6

Table 3. Geochemical data (major and trace elements) from whole rock analyses of 31 samples.

Sample		1	2	3	4	5	6	7	a1	a2	a3	a4	a5	a6	a7	a8	a9	a10
Original sample code		n/a	n/a	n/a	n/a	n/a	n/a	n/a	FET4H	TRU6FL	FET4	TRU6DY	FET4G	LBOD16	CUKR3	IKUCH7	NCHA21	MCHA21
Sampling latitude (º)		44.900	44.689	44.416	44.410	44.636	44.558	44.806	44.915	44.786	44.915	44.786	44.915	44.785	44.900	44.780	44.613	44.613
Sampling longitude (º)		34.141	34.322	99.978	33.873	34.389	33.952	34.045	34.176	33.994	34.176	33.994	34.176	33.992	34.142	34.029	34.346	34.346
Rock type		andesite	basaltic andesite	basalt	basalt	rhyolite	basaltic andesite	andesite	andesitic basalt	andesitic basalt	grano-diorite	basalt	andesite	basalt	alkali-syenite-monzonite	(trachy-) andesite	rhyolite	rhyolite
Major elements																		
SiO2	(%)	59.09	52.48	33.34	46.97	71.88	52.95	57.02	50.79	53.55	59.43	51.00	56.78	48.90	56.54	57.01	70.45	68.12
TiO2	(%)	1.25	0.76	0.65	0.71	0.14	0.74	0.71	1.13	0.70	1.40	0.79	1.58	0.63	1.21	0.68	0.30	0.29
Al2O3	(%)	14.78	18.08	13.76	15.71	14.19	16.15	17.71	16.33	18.90	13.91	21.32	14.38	15.48	15.31	18.60	15.56	14.97
Fe2O3	(%)	9.99	9.53	9.02	9.03	3.39	10.25	8.33	10.93	9.61	10.54	8.63	12.02	8.81	10.93	8.44	5.15	4.97
MnO	(%)	0.14	0.16	0.24	0.20	0.12	0.16	0.12	0.19	0.17	0.15	0.12	0.14	0.34	0.14	0.19	0.14	0.14
MgO	(%)	4.23	5.72	2.18	5.10	0.17	10.23	3.33	8.60	4.69	3.38	3.20	2.81	4.56	5.36	2.61	0.45	0.41
CaO	(%)	4.87	8.22	38.07	17.23	1.95	5.00	7.33	6.61	8.22	3.70	8.01	5.45	17.95	3.75	7.07	3.31	3.64
Na2O	(%)	5.48	3.98	0.75	2.87	5.22	4.58	3.48	4.57	3.17	5.67	4.81	6.11	1.56	5.47	3.74	4.77	4.40
K2O	(%)	0.35	0.54	0.01	0.28	1.22	0.12	0.62	0.61	0.57	0.10	1.22	0.18	0.36	0.45	1.00	1.30	1.20
P2O5	(%)	0.10	0.09	0.15	0.10	0.05	0.11	0.10	0.16	0.07	0.13	0.09	0.16	0.07	0.11	0.26	0.10	0.10
BaO	(%)	0.01	0.02	0.00	0.09	0.02	0.02	0.02	0.06	0.01	0.00	0.02	0.00	0.02	0.01	0.04	0.02	0.02
MgO+CaO	(%)	9.10	13.94	40.25	22.33	2.12	15.23	10.66	15.21	12.91	7.08	11.21	8.26	22.51	9.11	9.68	3.76	4.05
sum	(%)	100.28	99.59	98.18	98.29	98.35	100.32	98.75	99.97	99.67	98.41	99.19	99.60	98.67	99.28	99.63	101.53	98.25
LOI	(%)	3.42	4.06	20.07	13.16	2.36	4.90	2.11	4.49	1.40	4.70	3.96	5.49	10.14	2.68	2.35	3.50	4.16
Trace elements																		
V	ppm	324	262	282	260	6	258	198	329	303	323	288	348	283	315	80	15	16

Cr	ppm	12	41	27	429	7	353	6	168	13	9	8	3	648	23	6	4	4
Co	ppm	34	36	24	36		43	20	41	25	42	23	32	48	32	13	5	4
Ba	ppm	41	135	21	800	190	173	141	504	115		149	2	156	38	311	188	205
Sc	ppm	28	31	47	39	7	29	22	32	29	31	27	32	41	29	15	15	16
Ga	ppm	15	16	27	15	16	15	18	15	17	13	18	14	15	13	15	17	17
Zn	ppm	67	75	63	78	76	102	78	71	81	79	67	83	75	75	72	89	78
Cu	ppm	12	20	48	57	1	63	11	116	35	42	51	16	91	37	3	2	1
Ni	ppm	10	18	20	119	4	107	5	46	7	13	9	5	195	16	4	5	6
Mo	ppm					1	1	1	2	2	3	2	2	2	3	2	3	3
Nb	ppm	1.6		1.0		2.6		1.2	2.5	1.1	1.5		1.6	1.2	1.6	3.3	3.3	3.3
Y	ppm	28	17	15	12	35	16	24	18	20	34	18	40	15	28	21	37	36
Zr	ppm	85	47	43	40	152	46	64	52	44	92	45	104	35	82	88	137	136
Sr	ppm	121	240	74	445	109	276	188	451	255	45	488	85	210	137	357	196	125
Rb	ppm	4.1	14.8		6.3	35.7	3.2	11.7	19.5	9.3	2.8	24.7	6.5	7.5	5.8	35.9	36.8	33.9
Th	ppm		1.2	2.4	1.6	4.5	2.0	1.3						1.1		2.2	3.9	4.2
Pb	ppm				1.1	7.7	2.5	1.8	1.3	3.3	2.2	5.2		4.4	1.1	3.6	6.6	5.9
La	ppm		3.9	9.7	6.4	15.9	6.0	6.2	9.3	2.7	3.4	5.8	3.8	4.7	1.1	11.3	13.9	13.7
Ce	ppm	12.4	14.2	21.1	6.7	44.0	11.3	18.7	17.4	10.8	14.6	12.9	11.6	4.4	11.0	32.1	38.9	35.6
Pr	ppm	2.8	3.0	3.4	2.1	5.5	2.8	3.3	3.4	2.5	3.3	3.1	3.2	1.8	2.6	5.4	5.7	5.1
Nd	ppm	10.2	9.8	13.8	5.0	21.0	9.3	12.1	11.1	9.7	12.1	10.3	9.2	6.8	8.2	17.9	20.7	17.5
Sm	ppm	2.8	2.7	2.5	1.6	4.1	2.5	2.7	2.9	2.3	3.3	2.7	3.3	2.2	2.7	3.7	3.7	3.1

Sample		a11	a12	a13	a14	a15	a16	a17	a18	a19	a20	a21	a22	a23	a24
Original sample code		04CRPET	04KAR1	PAR2	OCHA21	KARSD	04CRLEB	FET4B	KARS2	04CRPAR	04KAR2	KIZ41	KA28b	KA28b	04KAR3
Sampling latitude (º)		44.900	44.913	44.833	44.613	44.934	44.752	44.915	44.934	44.833	44.918	44.806	44.913	44.913	44.918
Sampling longitude (º)		34.142	35.225	34.073	34.346	35.232	34.055	34.176	35.232	34.073	35.213	34.045	35.205	35.205	35.209
Rock type		andesite	(basaltic) andesite	trachyte	rhyolite	rhyolite (nuée ardente)	andesite	andesitic basalt	rhyolite (nuée ardente)	andesite	rhyolite	andesite	trachyte	trachyte	rhyolite
Major elements															
SiO2	(%)	57.16	58.05	64.98	68.90	76.12	46.32	54.87	75.13	65.98	69.06	58.95	70.20	66.37	69.17
TiO2	(%)	1.01	0.88	0.36	0.30	0.09	1.24	1.09	0.09	0.36	0.85	0.81	0.69	0.65	0.68
Al2O3	(%)	16.51	17.75	16.91	15.84	11.62	16.98	16.02	12.23	17.21	13.27	17.76	14.46	16.29	15.19
Fe2O3	(%)	9.70	7.30	4.35	5.20	0.84	10.93	10.45	0.82	4.38	5.63	7.54	3.54	4.35	3.05
MnO	(%)	0.14	0.15	0.15	0.14	0.04	0.19	0.19	0.07	0.14	0.26	0.08	0.11	0.17	0.12
MgO	(%)	4.97	2.92	1.57	0.47	0.36	9.85	7.64	0.37	1.48	0.86	2.74	0.37	0.78	0.38
CaO	(%)	4.44	9.06	4.13	3.13	1.52	12.76	2.89	1.27	4.34	1.40	5.60	4.04	5.66	2.01
Na2O	(%)	4.90	2.74	5.01	3.89	3.61	1.64	6.47	2.87	4.58	7.23	3.65	3.79	3.63	7.54
K2O	(%)	0.65	0.31	1.09	1.13	1.92	0.49	0.12	3.91	1.65	0.20	1.52	1.51	1.75	1.30
P2O5	(%)	0.11	0.23	0.12	0.11	0.02	0.29	0.10	0.01	0.12	0.32	0.15	0.23	0.22	0.25
BaO	(%)	0.01	0.01	0.03	0.02	0.04	0.03	0.01	0.04	0.05	0.00	0.02	0.08	0.05	0.03
MgO+CaO	(%)	9.41	11.98	5.70	3.60	1.88	22.61	10.53	1.64	5.82	2.26	8.34	4.41	6.44	2.39
sum	(%)	99.61	99.40	98.69	99.11	96.17	100.73	99.84	96.81	100.28	99.08	98.81	99.01	99.91	99.72
LOI	(%)	4.20	2.11	2.82	4.29	5.79	7.13	2.82	4.76	2.98	1.25	1.35	0.56	1.12	1.19
Trace elements															

V	ppm	298	296	59	17	4	353	292	3	56	150	123	71	105	44
Cr	ppm	29	6	1	4		583	43		2	9	37	3	9	2
Co	ppm	26	19	9	5	1	51	40	2	8	10	13	7	6	6
Ba	ppm	113	114	277	200	370	287	49	367	429	16	179	699	434	219
Sc	ppm	27	27	10	15	2	38	34	2	10	21	23	16	18	14
Ga	ppm	19	17	15	19	9	17	16	9	15	9	18	14	16	8
Zn	ppm	82	78	68	82	34	81	68	44	64	111	86	68	63	88
Cu	ppm	31	68	3	1	1	58	33		2	6	11	5	8	2
Ni	ppm	15	8	4	5	5	196	25	5	5	5	16	5	5	5
Mo	ppm	3	2	3	3	3	2	3	3	3	3	3	3	3	3
Nb	ppm	2.2	1.7	1.6	3.2	2.1	3.4	1.1	2.1	1.7	3.7	3.0	3.5	3.1	3.4
Y	ppm	27	26	19	35	19	21	29	14	18	32	25	29	29	39
Zr	ppm	79	72	84	135	74	62	74	74	84	116	89	101	113	116
Sr	ppm	63	275	184	184	231	357	155	147	176	18	214	206	239	33
Rb	ppm	2.8	4.0	22.8	27.6	40.4	18.7	1.6	60.8	23.1	2.1	24.2	25.1	33.9	15.4
Th	ppm		2.5	1.5	4.2	7.1	1.3		7.1	2.0	5.3	2.0	3.3	4.3	4.2
Pb	ppm	2.9	5.6	5.3	4.7	8.8	1.6	0.7	7.5	5.3	14.8	6.6	5.6	7.8	8.8
La	ppm	7.8	14.6	9.5	12.9	17.7	12.4	2.4	15.0	11.7	17.2	9.2	15.3	18.6	14.3
Ce	ppm	16.5	35.4	24.9	37.9	34.2	24.4	9.3	27.2	23.8	49.7	22.2	35.8	43.7	38.0
Pr	ppm	3.5	4.8	3.5	5.4	4.2	3.7	2.5	3.3	4.0	6.1	4.1	4.9	5.9	5.4
Nd	ppm	10.3	17.2	13.0	20.3	13.5	14.9	10.0	10.6	13.5	26.1	12.6	14.8	20.8	19.4
Sm	ppm	2.9	3.4	2.1	3.5	2.0	4.0	2.7	1.3	2.4	4.5	2.8	2.8	3.8	3.7

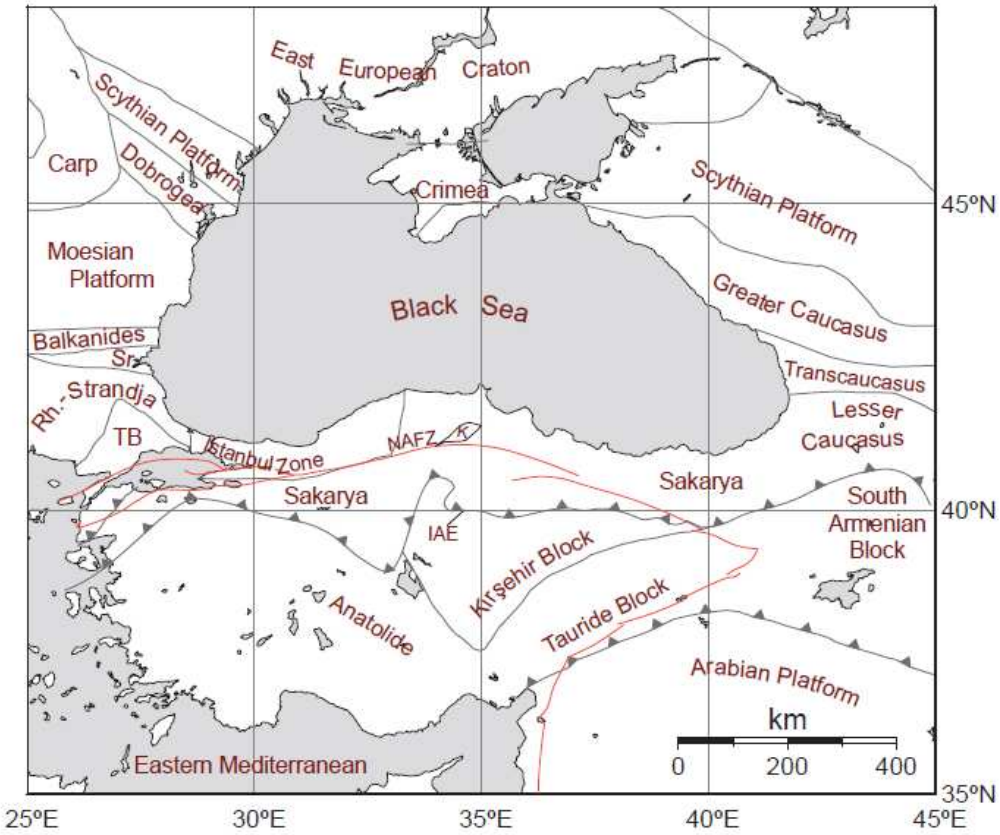

Figure 1

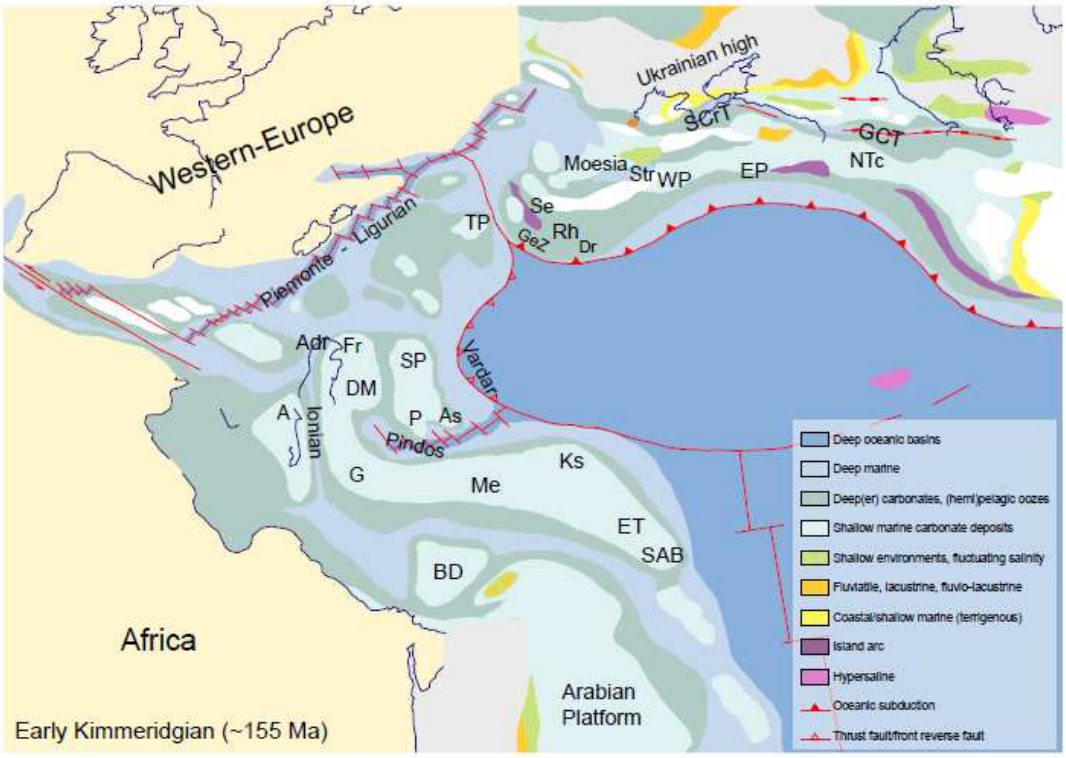

Figure 2

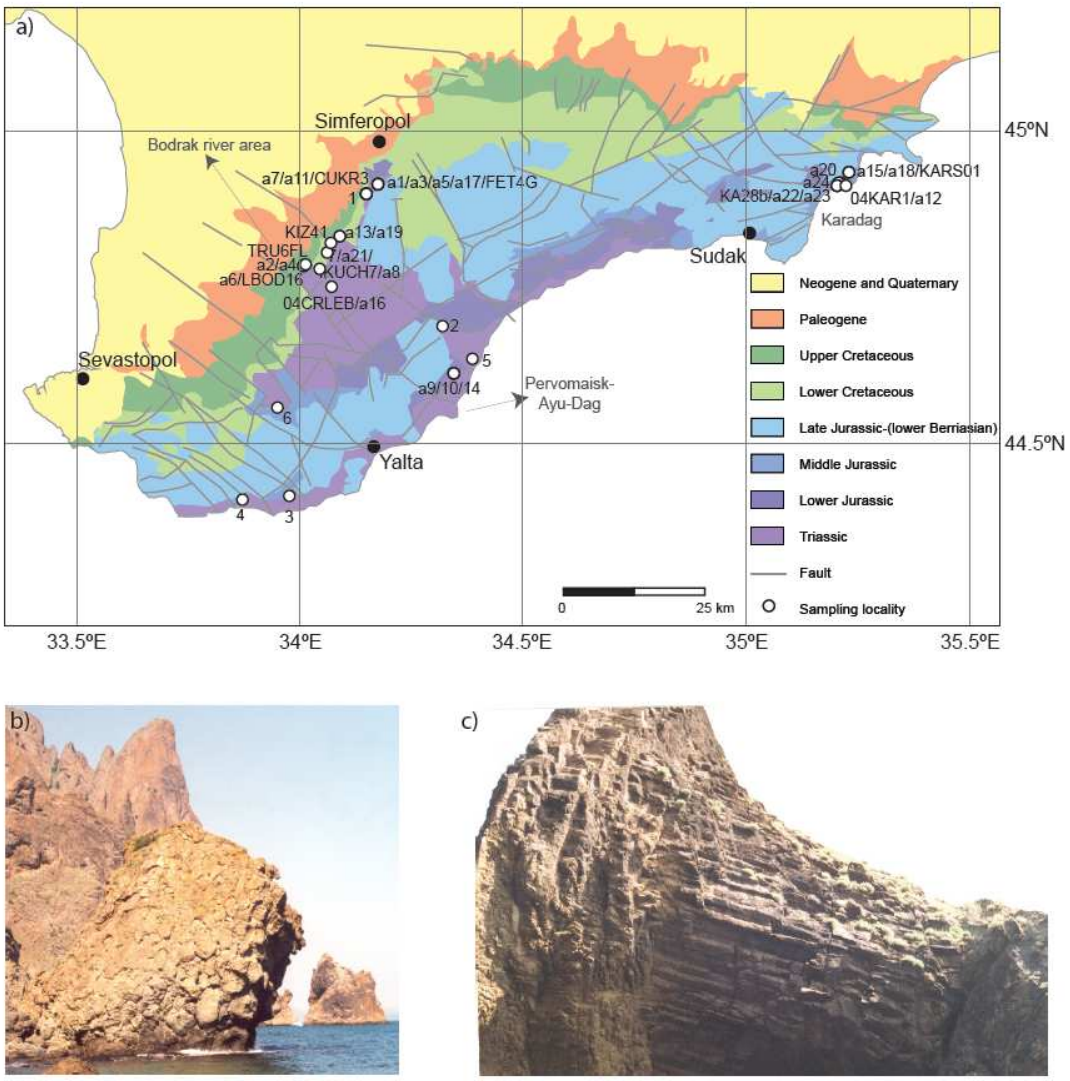

Figure 3

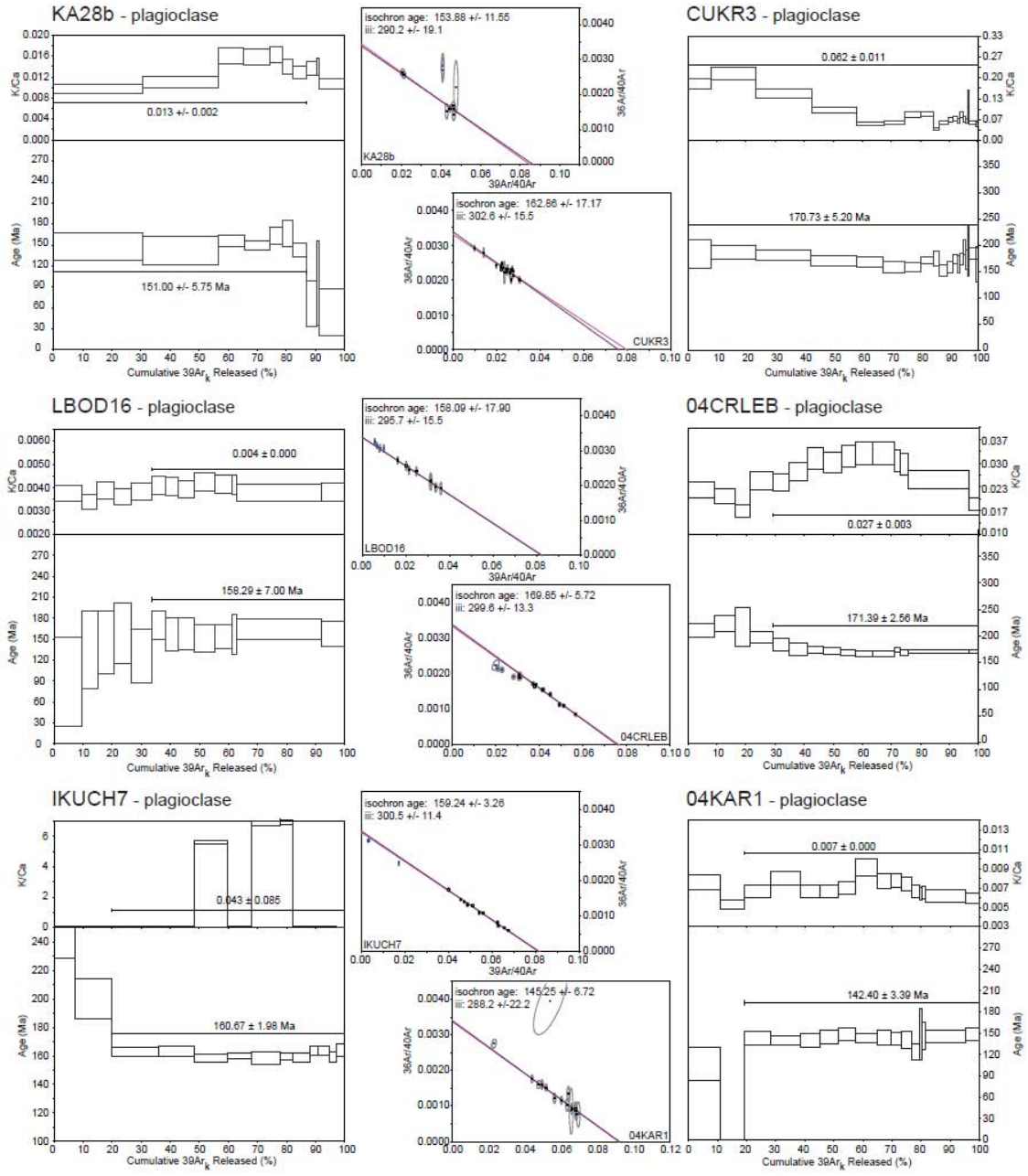

Fig. 4 (part A)

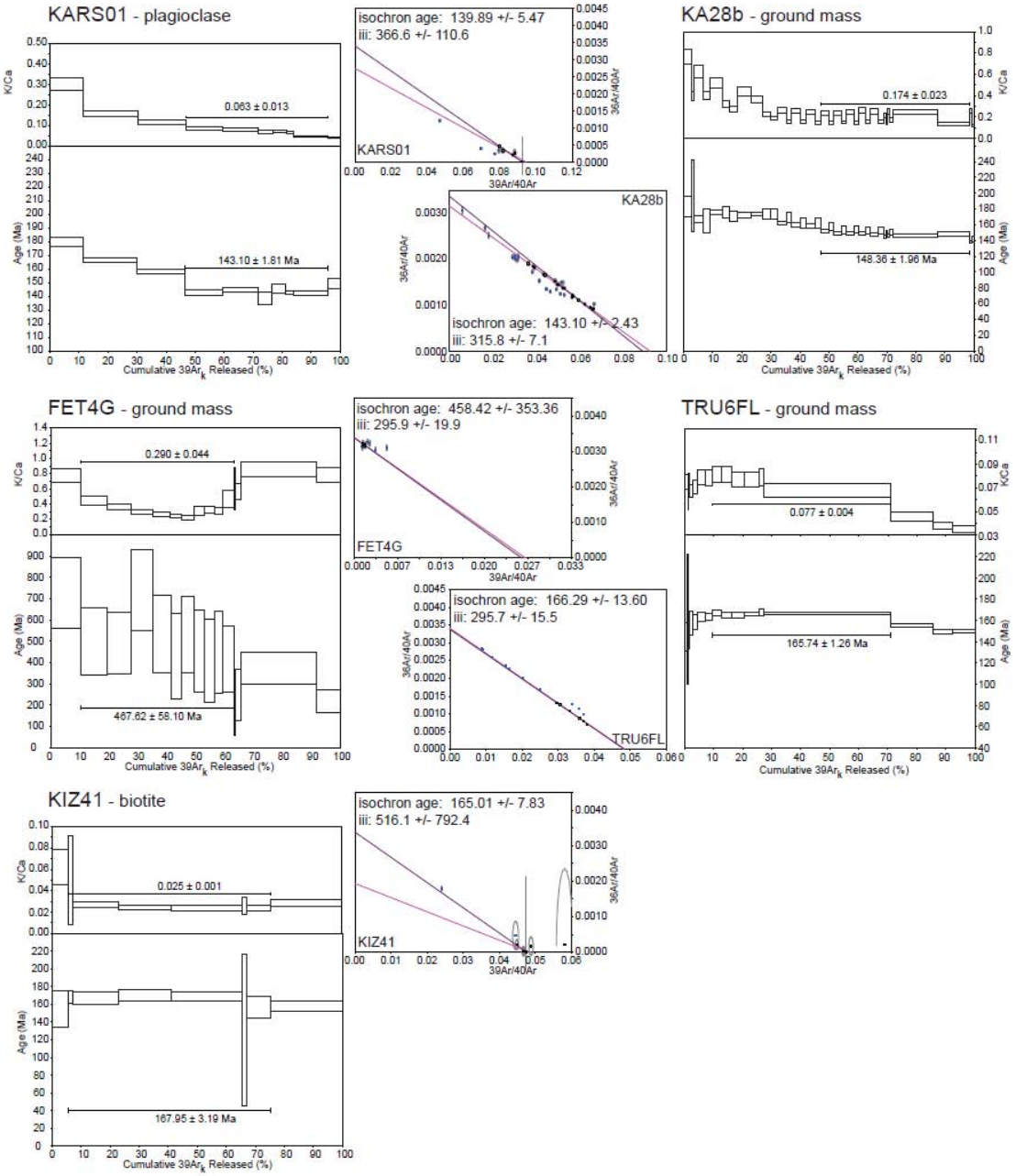

Fig. 4 (part B)

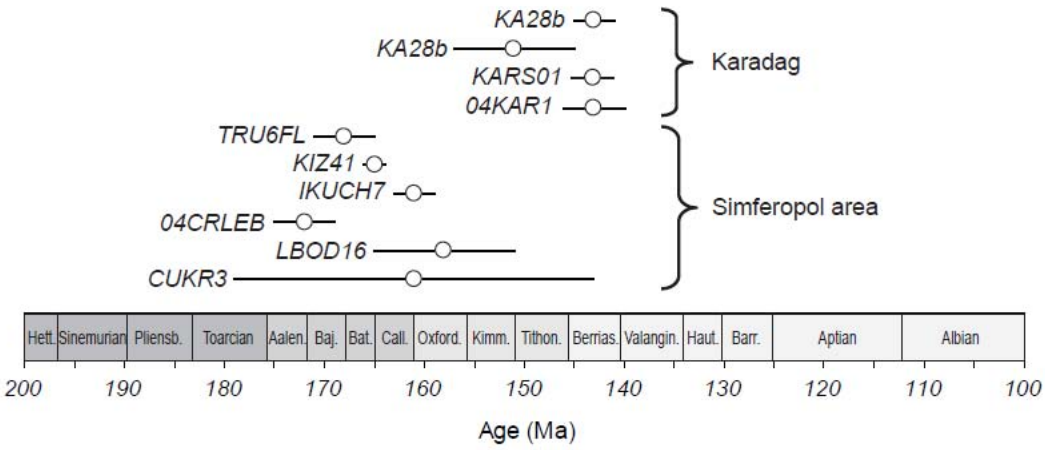

Figure 5

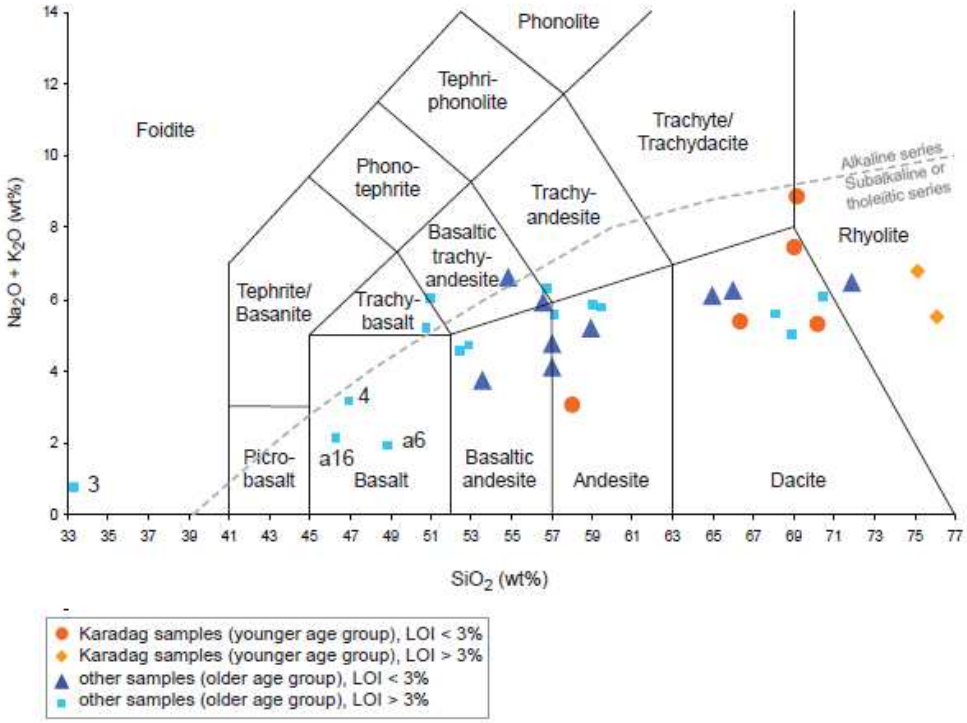

Figure 6

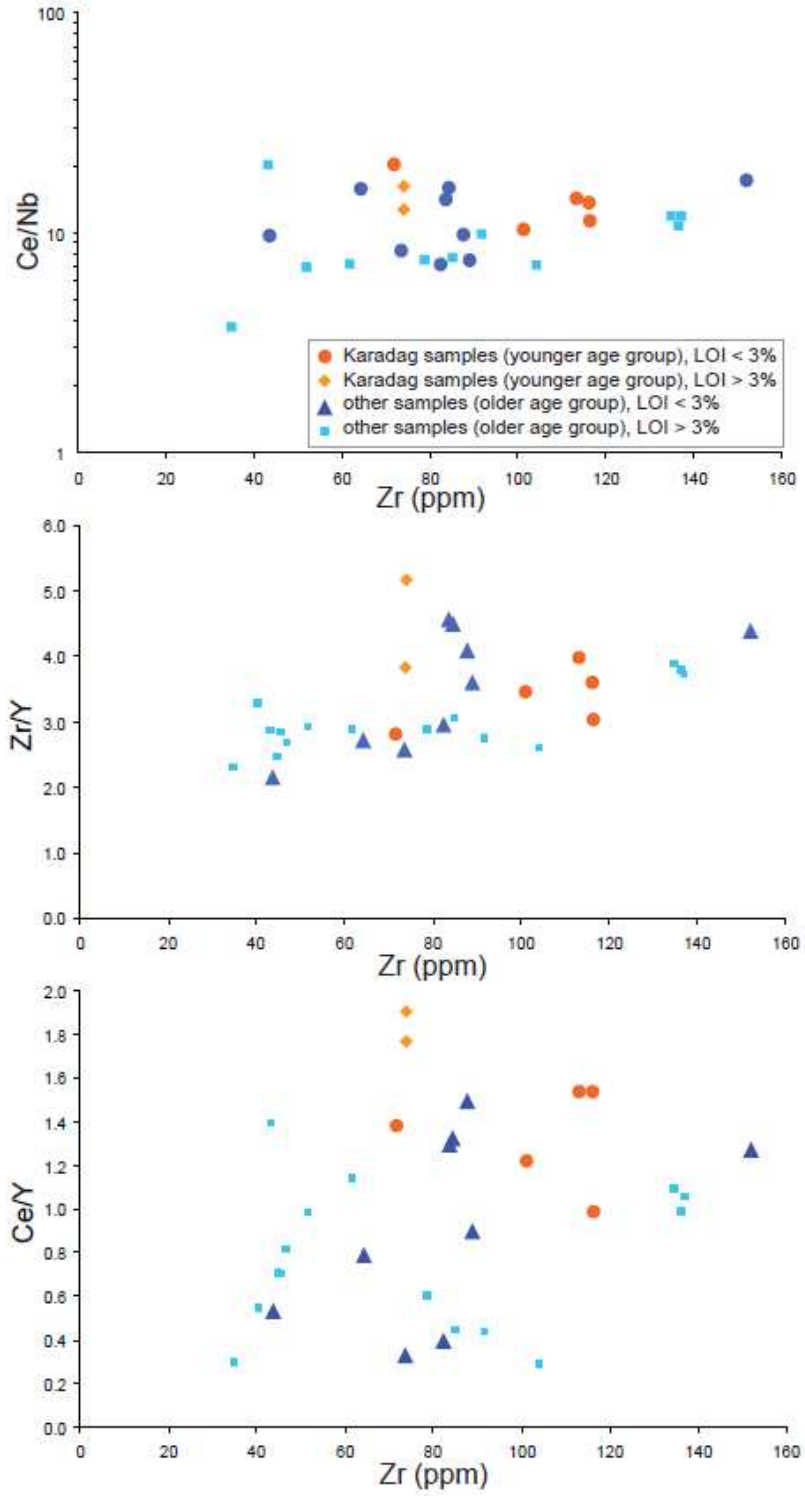

Figure 7

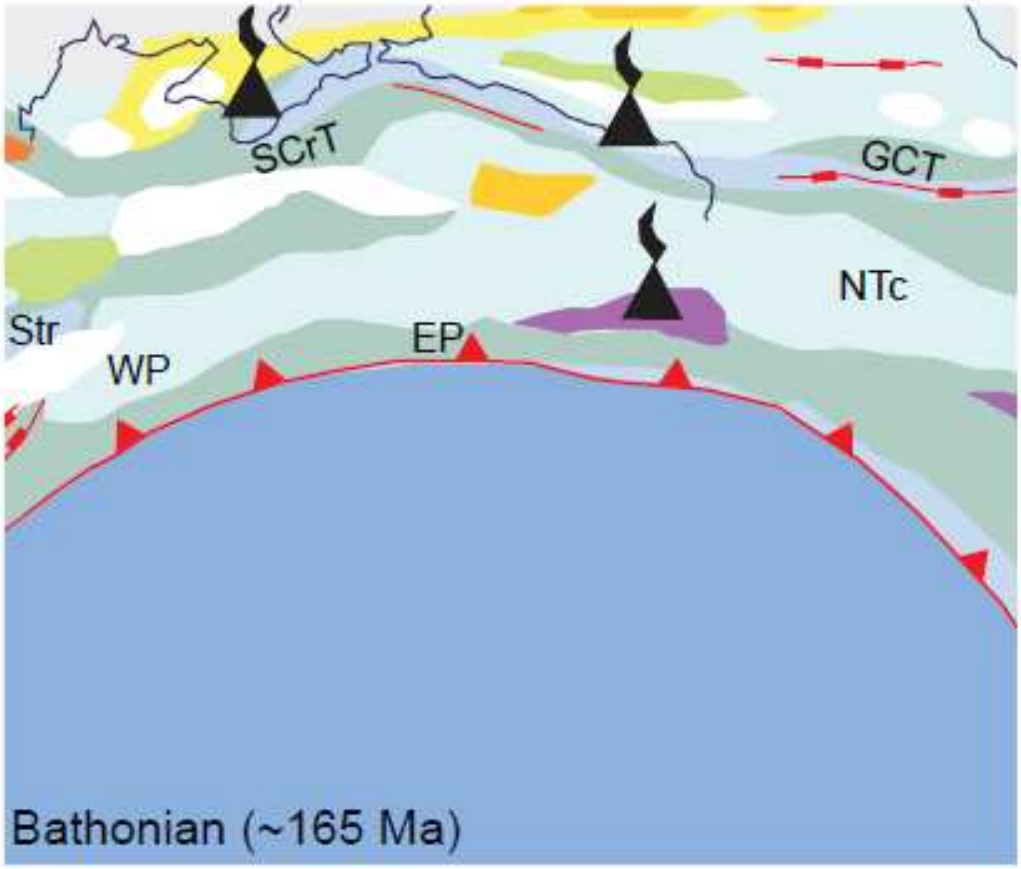

Figure 8a

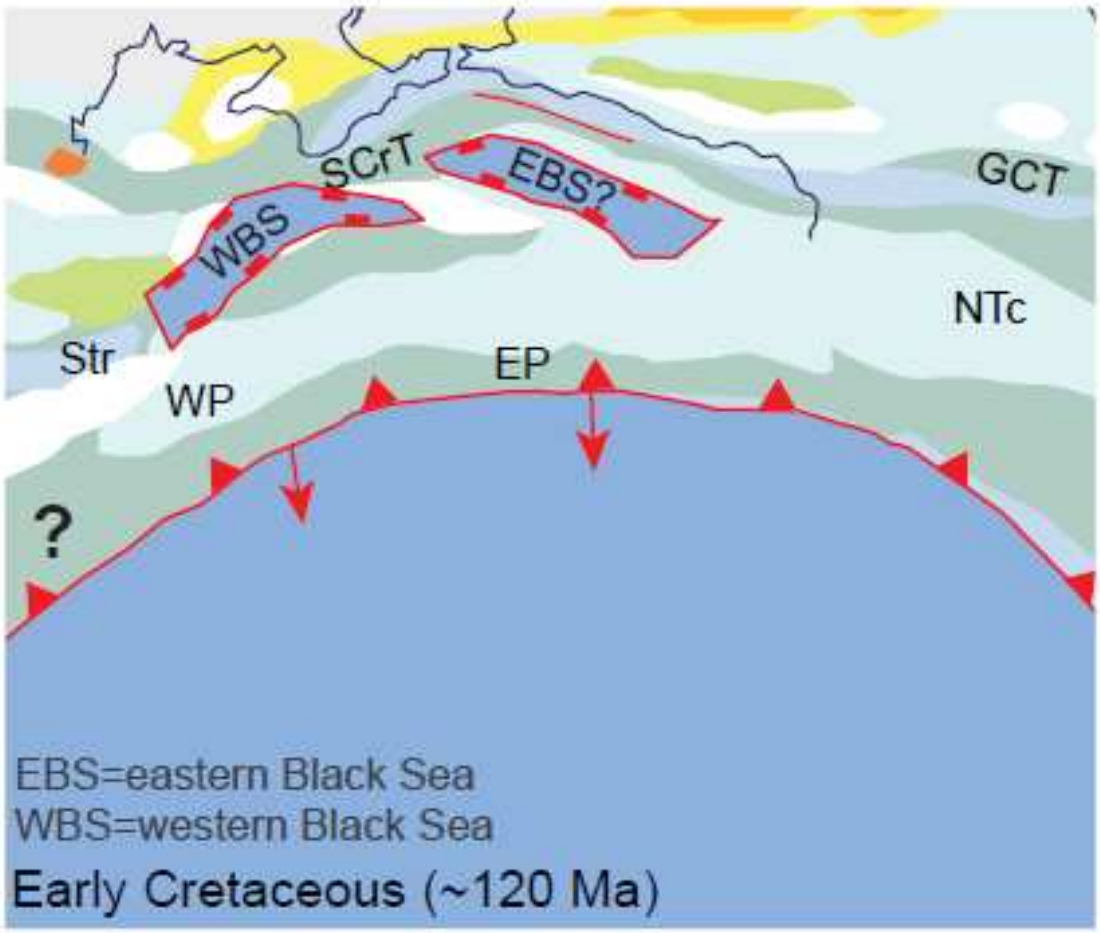

Figure 8b